

1 **Article Title**

2 Seismic Loss and Downtime Assessment of Existing Tall Steel-Framed Buildings and
3 Strategies for Increased Resilience

4 **Authors**

5 Carlos Molina Hutt, PE¹, M.ASCE

6 Ibrahim Almufti, SE², M.ASCE

7 Michael Willford³

8 Gregory Deierlein, PE⁴, F.ASCE

9 **Abstract**

10 In areas of high seismicity in the United States, the design of many existing tall buildings
11 followed guidelines that do not provide an explicit understanding of performance during
12 major earthquakes. This paper presents an assessment of the seismic performance of existing
13 tall buildings and strategies for increased resilience for a case study city, San Francisco,
14 where an archetype tall building is designed based on an inventory of the existing tall
15 building stock. A 40-story Moment Resisting Frame (MRF) system is selected as a
16 representative tall building. The archetype building is regular in plan and represents the state
17 of design and construction practice from the mid-1970s to the mid-1980s. Non-Linear
18 Response History Analysis (NLRHA) are conducted with ground motions representative of
19 the design earthquake hazard level defined in current building codes, with explicit
20 consideration of near-fault directivity effects. Mean transient interstory drifts and story
21 accelerations under the 10% in 50 year ground motion hazard range from 0.19% to 1.14%
22 and 0.15g to 0.81g respectively. In order to influence decision making, performance is
23 reported as the expected consequences in terms of direct economic losses and downtime.
24 Furthermore, to achieve increased levels of resilience, a number of strategies are proposed

¹ Teaching Fellow; University College London, Civil, Env. and Geomatic Engineering Dept.,
Chadwick Building, Gower Street, London, UK, WC1E6BT. Email: carlos.molinahutt@ucl.ac.uk

² Associate; Arup, Suite 700, San Francisco, CA, USA, 94105.

³ Principal, Arup Fellow; Arup, Suite 700, San Francisco, CA, USA, 94105.

⁴ Professor; Stanford University, Dept. of Civil and Env. Engineering, Blume Center, Building 540,
Stanford, CA, USA, 94305.

25 including seismic improvements to structural and non-structural systems as well as mitigation
26 measures to minimize impeding factors. Expected direct economic losses for the archetype
27 building are in the order of 34% of building cost and downtime estimates for functional
28 recovery are 87 weeks. The strategies presented in this paper enable up to a 92% reduction in
29 losses and minimize downtime for functional recovery to one day or less.

30 **Subject Headings**

31 Structural Analysis, Seismic Analysis, Non-linear Analysis, Steel Structures, Earthquake
32 Resistant Structures, Resilience, Losses, Downtime

33 **Text**

34 **Introduction**

35 Until the introduction of Performance Based Seismic Design (PBSD) in the 1990s, buildings
36 were designed using conventional building codes, which follow a prescriptive force-based
37 approach based on the first mode translational response of the structure (FEMA 2006).
38 Researchers and engineers have raised concerns that the prescriptive approach of building
39 codes is not suitable for tall building design due to the significant contribution of higher
40 mode effects (PEER 2010a). As a result of these shortcomings, several jurisdictions in areas
41 of high seismicity throughout the United States (e.g. Los Angeles and San Francisco) have
42 adopted a PBSD approach for the design of new tall buildings. While new designs follow a
43 more adequate approach, little is known about the seismic performance of older existing tall
44 buildings that were designed prior to the adoption of PBSD.

45 Tall buildings play a key role in the socio-economic activity of major metropolitan areas in
46 the United States. The resilience of these structures is vital in ensuring an effective recovery
47 after major disasters. Events such as the Canterbury earthquake in 2011 have highlighted the
48 impact of poor performing buildings on the business continuity of downtown districts, where
49 tall buildings are typically clustered together. Following the 2011 earthquake, Christchurch's

50 Central Business District (CBD) red zone covered a significant area of the city and more than
51 60% of the businesses were displaced (CERC 2012).

52 This paper presents an assessment of the seismic performance of existing tall buildings in a
53 case study city, San Francisco, where an archetype tall building is designed based on an
54 inventory of the existing tall building stock. The archetype tall building is representative of
55 the state of design and construction practice from the mid-1970s to the mid-1980s. A
56 performance assessment of the archetype building is conducted via NLRHA with ground
57 motions representative of the design earthquake hazard level defined in current building
58 codes and the associated direct economic losses and downtime are estimated from the
59 NLRHA results. Once the performance of the archetype building is assessed, a range of
60 structural and non-structural enhancements are explored for improved performance as well as
61 mitigation measures to minimize downtime.

62 The key differentiator of the work here presented is that it explicitly considers downtime
63 and recovery in the assessment methodology. This work goes beyond damage and direct
64 losses to consider repair and recovery times. Overall, the main contribution of this paper is
65 that it benchmarks the performance of an archetype tall building considering damage, direct
66 losses (due to repair or replacement), impact on building function and recovery of building
67 function. Furthermore, it evaluates ways of improving resilience by reducing damage and
68 taking other measures to improve recovery. Previous studies have assessed the performance
69 of existing steel moment frame buildings (Muto and Krishnan 2011, Gupta and Krawinkler
70 1999), but these studies were limited to 20 stories in height and focused on structural
71 performance assessment alone. Other studies have assessed the performance of new tall steel
72 moment frame buildings up to 40 stories (Jayaram and Shome 2012) and estimated economic
73 losses associated with building performance (Shome et al. 2013), but employed simplified
74 single bay two-dimensional structural models that neglect torsional and biaxial effects and do

75 not enable the study of detailed retrofit schemes for enhanced performance. This work draws
76 a comparison of the direct economic loss estimate results for the archetype building and those
77 presented in Shome et al. (2013) for a similar building typology designed to current
78 standards.

79 **Methodology**

80 The Structural Engineers Association of Northern California (SEAONC) Committee on
81 PBSD of Tall Buildings developed an inventory of the existing tall building stock in San
82 Francisco. This committee identified more than 90 buildings of 20 stories or greater, most of
83 which employed a steel moment frame lateral system. In order to assess the seismic
84 performance of existing tall buildings in San Francisco, NLRHA of a representative 40-story
85 building are carried out using the software package LS-DYNA (2013), which accounts for
86 both non-linear material and geometric effects. The three-dimensional analysis employs
87 robust non-linear component models to represent fracture of the welds, flexibility of the panel
88 zones, degradation of the plastic hinges, tensile and flexural capacity of the column splices
89 and buckling of the columns.

90 Near-fault directivity effects are explicitly considered in the Probabilistic Seismic Hazard
91 Analysis (PSHA) due to the close proximity of active faults to San Francisco's downtown
92 district, where most of these tall buildings are located. Twenty-two ground motion pairs are
93 selected and scaled following a methodology recently implemented for the design of a peer
94 reviewed high rise building in downtown San Francisco (Almufti et al. 2013). Such motions
95 are representative of the design earthquake hazard level defined in current building codes
96 (ASCE 2010) or if expressed in probabilistic terms have 10% chance of occurring over a 50
97 year period. The selected intensity level is also representative of the "expected earthquake"
98 defined by the San Francisco Planning and Urban Research Association (SPUR) for the
99 purpose of defining resilience. This "expected earthquake" corresponds to a 7.2 earthquake

100 scenario, which is an event that can be expected conservatively, but reasonably within the
101 lifetime of a structure (SPUR 2012).

102 The United States Federal Emergency Management Agency (FEMA) P-58 Performance
103 Assessment Calculation Tool (PACT) is used in order to assess the probable seismic
104 performance in terms of direct economic losses based on its site, structural, non-structural
105 and occupancy characteristics (FEMA 2012). Conceptual retrofit schemes include structural,
106 non-structural or a combination of these enhancements in order to provide enhanced
107 performance. Structural enhancements schemes include the introduction of an elastic spine
108 throughout the building core with steel bracing and the introduction of base isolation at
109 ground level. Non-structural enhancements introduce building components that are more
110 resilient to earthquake damage. All structural schemes (archetype or baseline, elastic spine
111 and base isolation) are assessed with standard and enhanced non-structural components.
112 Additionally, in order to provide a quantitative measure of resilience, downtime estimates for
113 re-occupancy and functional recovery are reported for all schemes based on the Resilience-
114 based Earthquake Design Initiative (REDi) guidelines (Almufti and Willford 2013).

115 Since the impact of the schemes considered on the overall resilience of the archetype building
116 is measured in terms of losses and downtime, a brief literature review on loss and downtime
117 assessment as well as resilience quantification is presented. The works referenced are not
118 exhaustive, but are presented to set the context of this work and how it draws and builds on
119 current best practice.

120 *Loss Assessment*

121 In the late 1980s, well founded loss estimation methods began to be employed in the
122 insurance industry and in the 1990s, these were supported by FEMA through the
123 development of the HAZUS earthquake loss estimation software. These developments were
124 primarily directed to the insurance and re-insurance industry (Khater et al. 2002) as HAZUS

125 attempts to address regional impacts of earthquakes. Numerous researchers have since
126 developed approaches to improve loss-estimating methods for individual buildings (Comerio
127 2006). For instance, Porter and Kiremidjian (2011) proposed a methodology to evaluate the
128 seismic vulnerability of buildings on a building specific basis, which estimates repair cost and
129 repair duration by treating the building as a collection of standard assemblies with
130 probabilistic fragility. Miranda and Aslani (2003) proposed including a probabilistic seismic
131 structural response analysis as a main step in the loss evaluation, enabling the assessment of
132 building specific loss estimation to be expressed probabilistically. These methodologies have
133 been integrated into PBSD of buildings through the FEMA P-58 (2012) project, which
134 enables estimates of direct losses attributable to earthquake damage to an individual building
135 and its contents, as well as the repair or reconstruction time. Unlike previous versions of
136 PBSD, the FEMA P-58 method enables measuring seismic performance through economic
137 losses, which can be understood by decision makers, rather than over methods that report
138 discrete performance levels (Krawinkler and Miranda 2004). Performance is directly related
139 to the damage a building may experience and the consequences of such damage such as loss
140 of use, repair and reconstruction costs (FEMA 2012). The methodology divides the
141 performance assessment into a number of elements that can be resolved rigorously and
142 consistently: earthquake intensity measures, engineering demand parameters, damage
143 measures and decision variables (Moehle and Deierlein 2004).

144 *Downtime Assessment*

145 The main challenge in quantifying downtime are the uncertainties associated with availability
146 of labor, materials, capital and relating damage and repair needs in building components with
147 lack of functionality (Krawinkler and Miranda 2004). The HAZUS method earlier discussed
148 includes a subroutine for calculating downtime. However, this downtime estimate is derived
149 from the direct economic loss estimate. Recognizing this essential component of loss

150 modeling, Comerio (2006) identifies various factors that affect building downtime and
151 divides components contributing to downtime into so-called “rational” and “irrational”
152 components. Rational components are those related to repair work whereas irrational
153 components are those related to resource mobilization. PACT provides an estimate of repair
154 time by combining damage states with probability distributions to represent repair duration.
155 These attempts are aimed at estimating repair time, which is only a small component of
156 overall downtime. More recently, the REDi guidelines propose a detailed downtime
157 assessment methodology by accounting for both direct repairs and impeding factors
158 (analogous to Comerio’s rational and irrational components), where estimates of the different
159 components that contribute to downtime are expressed probabilistically. The REDi guidelines
160 also account for utility disruption in the downtime assessment methodology. Even though
161 utility disruption is an important contributor to downtime, in the present study it does not
162 control over other impeding factors in the overall downtime assessment.

163 *Resilience Quantification*

164 Seismic resilience describes the loss and loss recovery required to maintain the function of a
165 system with minimal disruption (Cimellaro et al. 2006). A resilient system is one that
166 illustrates reduced failure probabilities, reduced consequence from failures (loss of life,
167 damage, etc.) and reduced recovery time (restored functionality) (Bruneau and Reinhorn
168 2006). Studies such as Bruneau et al. (2003), Cimellaro et al. (2006) and Bruneau and
169 Reinhorn (2006) offer a definition of resilience to cover all actions that minimize losses from
170 hazard, considering mitigation and recovery, making it possible to relate probability
171 functions, fragilities, and resilience in a single integrated approach such that resilience can be
172 quantified. Cimellaro et al. (2010) present these resilience concepts in a unified terminology
173 for a common reference framework for quantification of disaster resilience by means of
174 resilience functions, which provide a comprehensive understanding of damage, response, and

175 recovery as they illustrate the time variation of damage as well as its relationship to response
176 and recovery. Within this framework, a number of studies have explored the seismic
177 resilience of different systems such as healthcare facilities (Bruneau and Reinhorn 2007),
178 water resource systems (Wang and Blackmore 2009) or natural gas distribution networks
179 (Cimellaro et al. 2014).

180 This study expresses results in terms of losses and downtime. Even though the approach
181 followed in this work does not quantify resilience in absolute terms by means of a resilience
182 function, it provides a process to reach initial targets of functionality valid in achieving a
183 comprehensive resilience of structures (Bruneau and Reinhorn 2007). The results of this work
184 provide key indicators that enable discussions with stakeholders in order to increase the
185 resilience of existing buildings. This work demonstrates a relative increase in resilience from
186 a baseline performance (archetype existing building) through adoption of a range of structural
187 retrofits, non-structural enhancements and with mitigation measures which reduce or
188 eliminate disruptions in presence of earthquake events.

189 **Existing Tall Building Database**

190 The SEAONC Committee on Performance Based Design of Tall Buildings developed a
191 database of all buildings in San Francisco taller than 48.8 m (160 ft). The database tabulates
192 building characteristics by location, height, number of stories, year built and lateral system
193 type. Approximately 240 buildings greater than 48.8 m (160 ft) in height are identified. Fig
194 1a illustrates the number of tall buildings built each decade between 1900 and 2010.
195 Interviews with practicing engineers and a partial database gathered previously by the
196 SEAONC committee revealed information on the lateral system type for some of these
197 buildings. Information on the remaining buildings was obtained by viewing construction
198 documents available at the San Francisco Department of Building Inspection (DBI). The
199 database identifies the lateral system type for approximately 80 out of the 240 buildings. The

200 lateral system type of many buildings remains unknown because, while drawings of existing
201 buildings are made available for viewing at the DBI (California Health and Safety Code
202 19850), access to drawings is limited by the difficulty in locating relevant structural
203 information within the large microfilm archive.

204 In order to select a prototype building for this study, the data from the existing tall building
205 database was disaggregated. Fig 1b shows the lateral system type for tall buildings built
206 between 1960 and 1990. The sub-category ‘Other System’ means that the lateral system of
207 the building is known and it is not a steel moment frame, while the sub-category ‘Unknown
208 System’ is designated for all buildings for which the lateral system is unknown. This data
209 reveals that the steel Moment Resisting Frame (MRF) system was the most prevalent type in
210 pre-1990s construction for buildings greater than 35 stories in height. A sidewalk survey of a
211 random sample of these tall buildings revealed that most are regular in plan, though some
212 have setbacks up the height and others lack corner columns.

213 **Archetype Building**

214 A 40-story steel MRF was selected as a representative archetype tall building. The archetype
215 building is regular in plan and represents the state of design and construction practice from
216 the mid-1970s to the mid-1980s. Based on examination of existing building drawings, the
217 archetype building layout consists of: 38 levels of office space; 2 levels for mechanical
218 equipment (one at mid-height and one at the roof); 3 basement levels for parking; building
219 enclosure composed of precast concrete panels and glass windows; floor system composed of
220 concrete slab 76.2 mm (3 in) over metal deck 63.5 mm (2.5 in) supported by steel beams;
221 columns of A572 (50 ksi) steel and beams of A36 (36 ksi). As illustrated in Fig 2, the
222 prototype system consisted of a space frame with 6.1 to 12.2 m spans (20 to 40 ft) using wide
223 flange beams, built up box columns and welded beam-column connections. Typical story
224 heights are 3 m (10 ft) for basement levels, 6.1 m (20 ft) at ground level (lobby) and 3.8 m

225 (12.5 ft) for typical office levels. The overall height of the structure is 154.7 m (507.5 ft)
226 above ground and 9 m (30 ft) below grade.

227 The design of the prototype building follows the provisions of the Uniform Building Code of
228 1973 (UBC 1973) and the 1973 Structural Engineers Association of California (SEAOC)
229 Blue Book (SEAOC 1973), which was commonly employed to supplement minimum design
230 requirements. Based on discussions with engineers whose firm designed such buildings
231 (personal correspondence, H. J. Brunnier Associates), lateral wind forces generally governed
232 the design of tall buildings over seismic forces in the 1973 UBC, and member sizes would
233 have been sized for wind demand and detailed to provide a ductile response under seismic
234 excitation. While the 1973 UBC does not specify drift limits, design offices would have
235 implemented drift limits established by their firm's practice or those obtained from the
236 SEAOC Blue Book of the time. For this study, the drift limit recommendations from
237 Appendix D of the SEAOC Blue Book (1973) are used, equal to 0.0025 for wind and 0.005
238 for seismic for buildings taller than 13 stories. Current seismic drift limits are slightly more
239 stringent: 0.020 times the story height, which for a deflection amplification factor of 5.5 as
240 prescribed for special steel MRF, is approximately 0.004 (ASCE 2010). For the prototype
241 building, since wind drift limits governed the MRF section sizes, beams and columns have
242 low strength utilization ratios under code prescribed forces. The effective wind base shears
243 with the forces prescribed by UBC 73 are 2.17% in the long direction of the building and
244 3.25% in the short direction, whereas the overall effective seismic base shear is 2.06%.

245 Typical member sizes and connection details were verified against available existing building
246 drawings. Consistent with these records, built-up box columns and wide flange beams are
247 selected for the prototype building. A summary of the design section sizes of the steel MRF
248 are illustrated in Table 1. Fig 3 illustrates some of the typical details frequently observed in
249 existing building drawings. Since the switch in the weld process that led to welds with very

250 low toughness, as evidenced by fractures observed in the 1994 Northridge earthquake, took
251 place in the mid-1960s (FEMA 2000), it is assumed that that fracture prone pre-Northridge
252 moment connections are common. Designs of the 1970's did not include consideration of
253 panel zone flexibility or strong column-weak beam principles. Krawinkler's panel zone
254 model was not developed until 1978 (PEER 2010b) and strong column-weak beam
255 requirements were not introduced in the UBC provisions until 1988 (SAC 2000). Column
256 splices are typically located 1.2 m (4 ft) above the floor level approximately every three
257 floors. Observed typical splice connection details consist of partial joint penetration welds of
258 half the thickness of the smaller section being connected. When subject to tensile forces,
259 these splices can only carry a fraction of the moment capacity and/or axial tension capacity of
260 the smallest section size being connected. Furthermore, experimental tests on heavy steel
261 section welded splices have illustrated sudden failures with limited ductility (Bruneau and
262 Mahin 1990). Based on this evidence, column splice failures are considered in our
263 assessment.

264 **Analytical Model**

265 The component models to represent non-linear columns, beams, panel zones and splices are
266 described in this section. Concrete slabs are modeled as elastic cracked concrete 2D shell
267 elements to represent the flexible floor diaphragm. Columns are modeled as lumped plasticity
268 beam elements with yield surfaces capable of capturing interaction between bi-axial bending
269 moment and axial force. Buckling in compression is also captured. Degradation parameters
270 for response under cyclic loads are calibrated based on experimental tests of tubular steel
271 columns (Kurata et al. 2005) following the guidelines for tubular hollow steel columns under
272 varying levels of axial load (Lignos and Krawinkler 2010).

273 Beams that form part of the moment frames are modeled as lumped plasticity elements with
274 implicit degradation in bending to capture random fracture at the connections. The random

275 fracture model follows the methodology proposed by Maison and Bonowitz (1999), in which
276 the plastic rotation at which fracture occurs is a random variable characterized by a truncated
277 normal distribution following tests designed for typical pre-Northridge practice. Top and
278 bottom capacities are modeled as a single random variable with a mean plastic rotation
279 capacity of 0.006 radians and a standard deviation of 0.004 radians. The truncated tail at zero
280 plastic rotation denotes fracture prior to yield, which is supported by data from the SAC
281 studies (SAC 2000). When fracture prior to yield occurs, it is set at 70% of the moment
282 capacity of the beam. The residual moment capacity after fracture is set at 25% of the beam
283 capacity. For each of the analysis runs, subject to a unique earthquake record, a different
284 random fracture sample is assigned for each of the moment connections in the building
285 model. Therefore, all analysis runs for the archetype building model have a unique
286 distribution of plastic rotation capacities throughout the structure. However, when assessing
287 retrofit schemes, the distribution of plastic rotation capacities is consistent with the analysis
288 runs from the baseline building model to enable a direct assessment of performance
289 enhancement as a result of the retrofit measures adopted.

290 Panel zones are modeled using the Krawinkler model as outlined in PEER/ATC-72-1 (2010b)
291 by the use of an assembly of rigid links and rotational springs that capture the tri-linear shear
292 force-deformation relation. Since the prototype building model is three dimensional and
293 columns are built-up box sections, the shear force-deformation relationship in each direction
294 is assumed decoupled. Column splices are modeled as non-linear springs capable of reaching
295 their nominal capacity with a sudden brittle failure followed by 20% residual capacity when
296 subject to axial tension and/or bending. Full column capacity is assumed in compression
297 since this is achieved by direct bearing.

298 Analytical models are subject to ground motions in conjunction with expected gravity loads
299 associated with the seismic weight of the structure. Seismic weight includes self-weight,

300 superimposed dead load and 25% of the unreduced live loads. 2.5% damping is assumed in
301 the analysis (PEER 2010a). A fixed base is assumed at foundation level and soil-structure
302 interaction is not considered. Ground Motions are input at top of foundation level.

303 **Seismic Hazard and Ground Motions**

304 The majority of tall buildings in San Francisco are clustered in the downtown area, located
305 approximately 14 km from the San Andreas Fault and 16 km from the Hayward Fault. The
306 authors conducted a site specific PSHA at a representative site, near the San Francisco
307 Transbay Transit Center development, with subsurface ground conditions consistent with Site
308 Class D (as defined in ASCE 7-10 2010) for the 10% in 50 year hazard. The selected
309 intensity level is also representative of the “expected earthquake” defined by SPUR for the
310 purpose of defining resilience. This “expected earthquake” corresponds to a 7.2 earthquake
311 scenario, which is an event that can be expected conservatively, but reasonably within the
312 lifetime of a structure (SPUR 2012). Reference to such scenario earthquake is important as it
313 is a concept easier to grasp than probabilistic measures and therefore effective for
314 communicating risk to policymakers and the public.

315 Forward directivity effects are known to cause pulselike ground motions at near-fault sites.
316 Pulselike ground motions place extreme demands on structures and are known to have caused
317 extensive damage in previous earthquakes (Shahi and Baker 2011). Due to the site’s close
318 proximity to active faults, near-fault directivity effects are expected to significantly contribute
319 to the hazard. Therefore, a methodology proposed by Almufti et al. (2013), which is an
320 extension of the method proposed by Shahi and Baker (2011), is utilized to incorporate
321 velocity pulses in the selection of the design level ground motions for this study. This
322 methodology uses disaggregation information from the PSHA to construct a suite of target
323 spectra used for matching an appropriate proportion of pulselike motions with characteristics
324 (pulse amplitude and pulse period) representative of a desired hazard intensity level. This

325 methodology has been successfully implemented in the development of ground motions of a
326 peer-reviewed high rise project in San Francisco (Almufti et al. 2013).

327 A Conditional Mean Spectrum (CMS) approach is used to characterize short and long-period
328 ground motions separately (Baker 2011). Two suites of bedrock motions are developed to
329 cover the entire period range of interest from $0.2T_1$ to $1.5T_1$ as defined in ASCE 7-10 (2010),
330 where T_1 is the fundamental period of the structure. Each suite consists of 11 bidirectional
331 motions each. The short-period suite covers the range of periods from 0.5 to 4 seconds and
332 the long-period suite covers the range of periods from 4 to 10 seconds. The archetype
333 building has a fundamental period of approximately 5 seconds and therefore the period range
334 of interest from 1 to 7.5 seconds is bounded by the two suites of motions. A pulse-included
335 PSHA at bedrock is conducted at two conditioning periods, 0.75 seconds and 7.5 seconds,
336 which are selected to best facilitate covering the period range of interest accounting for
337 potential elongation of the fundamental period due to non-linearity of the archetype building
338 and the structural retrofit schemes considered. The disaggregation of the pulse-included
339 PSHA at the two conditioning periods reveals that approximately 20% of the short-period
340 ground motions (2 out of 11 ground motions) contributing to the hazard are pulselike while
341 approximately 80% of long-period ground motions (8 out of 11 ground motions) contributing
342 to the hazard are pulselike. Arup's in house software SISMIC (2012) is used to conduct the
343 pulse-included PSHA.

344 For each pulselike motion, a unique pulse-included CMS is developed as the target spectrum
345 for the pulse component of the ground motion using the method of Shahi and Baker (2011).
346 For non-pulselike motions, seed ground motions are selected based on disaggregation results,
347 linearly scaled to the target at the conditioning period, and then spectrally matched to the
348 conventional CMS, developed using epsilon correlations by Baker and Jayaram (2008). Once
349 the bedrock ground motions are developed, a non-linear site response analysis is conducted

350 using LS-DYNA (2013) in order to characterize soil shaking and obtain input motions for the
351 structural analysis. The soil profile and non-linear soil properties, which define the shear
352 modulus reduction curves utilized in the site response, were obtained from soil testing at the
353 representative site.

354 The maximum and minimum demand surface response spectra for each suite of motions are
355 shown in Fig 4. ASCE 7-10 (2010) requires that for site-specific ground motions the design
356 level response spectra is no less than 80% of the code prescribed design level spectrum. Fig 5
357 illustrates compliance with this criterion as the Envelope of the Mean of the Maximum
358 Demand (EMMD) surface response spectra for the short and the long-period motions is no
359 less than 80% of design level spectrum over the period range of interest of the structure
360 (shaded in grey) from 1 to 7.5 seconds. In order to meet this requirement, the scale factors
361 applied to the short and long-period suite of motions are 1.0 and 1.6 respectively. Fig 5 shows
362 that the EMDD is close to the 475 year probabilistic estimate of the hazard. These ground
363 motions are utilized to conduct an intensity based performance assessment of the archetype
364 building. The pulse components of the pulselike ground motions are applied evenly to each of
365 the principal directions of the building, i.e. out of 8 pulselike motions, 4 are oriented in one
366 direction while the other 4 are oriented 90 degrees from that direction. For non-pulselike
367 motions, the maximum demand orientation is random relative to the principal axes of the
368 structure.

369 **Building Performance Model**

370 Communicating performance as the probable consequences in terms of direct economic
371 losses to repair earthquake damage can influence decision making. Financial institutions use
372 quantitative statements of probable building repair cost expressed as a percentage of building
373 replacement value. The authors use this metric for our study, where the costs are expressed in
374 present dollars. Losses are expressed as a percentage of repair cost, i.e. the cost required to

375 restore a building to its pre-earthquake condition, over total building cost, i.e. the cost
376 required to rebuild with a new structure of similar construction. In this study, total
377 replacement cost includes replacement of basic building structure, exterior enclosure, MEP
378 (mechanical, electrical and plumbing) infrastructure as well as all tenant improvements and
379 contents. Demolition and site clearance are not included in the total replacement cost since
380 the intent is to estimate the direct losses. Based on a class 5 rough order of magnitude cost
381 estimate based on the Association for the Advancement of Cost Engineering (AACE), the
382 most likely estimated cost for the archetype building in San Francisco in present dollars is
383 \$330 per square foot with an accuracy range of -5% to +30% .

384 The building performance model is defined for this study as a model to assess the probability
385 of earthquake losses and downtime. The methodology followed for the loss and downtime
386 assessment is outlined in Fig 6 and described in more detail below. Strategies for increased
387 resilience are also presented. Lastly, modeling uncertainty, which is inherent to the loss and
388 downtime assessment methodologies, is also discussed.

389 *Loss Assessment Methodology*

390 Engineering demand parameters, including maximum interstory drift ratios and peak floor
391 accelerations are obtained from the NLRHA at every story in the building under
392 consideration. Fig 7 illustrates the input demand parameters for the archetype building and
393 each of the retrofit schemes obtained from the NLRHA results, which are well within the
394 limits currently specified in building codes such ASCE 7-10 (2010). These parameters are
395 used as input demands to the building performance model, which contains structural and non-
396 structural components at each story level for all components in the building that are
397 susceptible to earthquake damage. Structural component quantities are based on the structural
398 design of the archetype building. Non-structural component quantities are estimated based on
399 typical quantities found in buildings of similar occupancy by use of the Normative Quantity

400 Estimation Tool (FEMA 2012). Normative quantities are an estimate of the quantity of
401 components and contents likely to be present in a building of a specific occupancy based on
402 gross square footage. These quantities were developed based on a detailed analysis of
403 approximately 3,000 buildings across typical occupancies (FEMA 2012). This study assumes
404 estimates of quantities at the 50th percentile level. Where possible, these quantities were
405 verified with registered engineers for the validity and relevance of the components to a tall
406 building designed in the mid-1970s, and modified where discrepancies were identified.

407 Each one of these structural and non-structural building components has a component
408 fragility function. A component fragility function is a statistical distribution that indicates the
409 conditional probability of incurring damage at a given value of demand, which is typically
410 assumed to be lognormal distribution. Component fragility functions contain unique
411 fragilities for each possible damage state in the component. For instance, standard partition
412 walls, designated in Table 2 by fragility C1011.001a, have 3 possible damage states (DS):
413 DS1 consists on minor cracking of the wall board, DS2 consists on moderate cracking or
414 crushing of the wall boards typically around corners and DS3 consists on significant cracking
415 or crushing of the wall boards and buckling of studs (FEMA 2012). Each damage state has an
416 associated consequence function, from which the repair cost and repair time associated with
417 the level of damage in the component is estimated. The occurrence of damage states is
418 predicted by individual demand parameters, as determined from the NLRHA. For each
419 realization, fragility functions are used in conjunction with demand parameters to determine a
420 damage state for each component. Consequence functions are then used to translate damage
421 states into repair or replacement costs (FEMA 2012). The direct economic losses for each
422 realization are estimated by conducting this calculation for every component at every story
423 throughout the building. Table 2 summarizes components included in the standard building
424 performance model, including fragility number, category, quantities, units, demand parameter

425 (DP), number of damage states (NDS), as well as median (M), dispersion (D), mean repair
426 cost (MRC) and mean repair time (MRT) for the first damage state (DS1). For illustration,
427 one sample non-structural component included in the enhanced building performance model
428 is shown in parenthesis in Table 2 for each component category.

429 *Downtime Assessment Methodology*

430 While seismic loss estimates associated with direct economic losses enable discussions with
431 building owners and investors about how individual retrofit interventions can move buildings
432 in the direction of becoming more resilient, they do not provide a quantitative measure of
433 resilience. In addition to direct economic losses, there is great vulnerability to indirect
434 economic losses due to downtime, defined as the time required to achieve a recovery state
435 after an earthquake. The Structural Engineers Association of Northern California (SEAONC)
436 defines three recovery states: re-occupancy of the building, pre-earthquake functionality and
437 full recovery (Bonowitz 2011). Re-occupancy occurs when the building is deemed safe
438 enough to be used for shelter, though functionality may not be restored. Functional recovery
439 occurs when the building regains its primary function, i.e. it is operational. Lastly, full
440 recovery occurs when the building is restored to its pre-earthquake condition, it follows from
441 functional recovery once additional repairs for aesthetic purposes have been completed.

442 The REDi guidelines provide a detailed downtime assessment methodology for individual
443 buildings and identify the likely causes of downtime such that these can be mitigated to
444 achieve a more resilient design. The methodology identifies the extent of damage and
445 criticality of building components that may hinder achieving a recovery state through the
446 introduction of repair classes. Repair classes are assigned to the each damage state for each
447 building component. Repair classes dictate whether the damage in the component hinders
448 building re-occupancy, functional recovery or full recovery. If the damage in any component
449 hinders achieving a certain recovery state, the component needs to be repaired before such

450 recovery state can be achieved. Once the components that need repairing in order to achieve a
451 certain recovery state have been identified, the methodology includes delay estimates
452 associated with impeding factors, defined as those factors which may impede the initiation of
453 repairs. Impeding factors include post-earthquake inspection, engineering mobilization,
454 contractor mobilization, financing, permitting and long-lead time components. Following an
455 earthquake, a building owner is expected to submit an inspection request if the structural
456 integrity of the building is in question. Furthermore, the jurisdiction, tenants or insurance
457 companies may also request an inspection regardless of the extent of damage. Following
458 post-earthquake inspection, as illustrated in Fig 6, there are three distinct sequences of delays
459 due to impeding factors, the longest of which controls and is used in the downtime estimate.
460 The first sequence of delays is related to engineering mobilization, review or re-design and
461 permitting. This accounts for the time required to engage an engineer for structural
462 assessment if there is structural damage to the building, perform relevant structural
463 calculations, as well as re-design and issue drawings depending on the level of damage to the
464 structure. The second sequence of delays concerns contractor mobilization. The time required
465 to mobilize a contractor is dependent on a number of factors such as the severity of damage,
466 bidding or building height among others. Furthermore, the mobilization of a contractor to
467 conduct repair work on tall buildings is dependent on the availability of tower cranes. In
468 addition to contractor mobilization, long lead components are a key consideration of
469 downtime. These components are not readily available in normal circumstances or are custom
470 made. The repair schedule can be significantly impacted by long lead components as these
471 items cannot be replaced until they have arrived on site. The last sequence of delays is related
472 to financing. The lack of financing to fund repair work can result in significant delays. If the
473 losses associated with earthquake damage exceed the funds available to fund repair work,

474 additional sources of funding need to be sought out. The delays associated with securing such
475 funds are dependent on the method of financing e.g. private loan versus insurance.

476 Following any delays associated with impeding factors, repair work can commence. The
477 REDI guidelines provide a logical approach for labor allocation and repair sequencing of
478 structural and non-structural components on a floor per floor basis. The repair sequence
479 defines the order in which repairs take place. As illustrated in Fig 6, structural repairs need to
480 be conducted at any given floor before repairs to other building components at that level (or
481 above) can commence. Non-structural repairs are divided into the following categories:
482 egress (stairs and elevators), façade (exterior partitions and cladding), MEP and office fitouts
483 (heating, ventilation and air conditioning -HVAC, partitions and ceiling tiles). Once structural
484 repairs at any given floor are complete, repair of non-structural components can commence,
485 in parallel, following a rational approach, e.g. repair of interior partition walls cannot
486 commence until HVAC ducts have been repaired. Overall repair time is estimated based the
487 repair times dictated by PACT, which are expressed in number of days for a single worker to
488 complete the work and the labor allocation for each floor in the building. Table 3 illustrates
489 the labor allocation parameters employed in the repair work estimates. To account for
490 subcontractor resource limitations, the number of workers repairing a certain type of
491 component is limited. Such limit is also included in Table 3. Furthermore, the total number of
492 workers in the building is also limited by the number of workers allocated to a project.

493 Following discussions with contractors and cost estimators, the REDI guidelines define the
494 total number of workers on the project as a function of the square footage of the building,
495 which for the archetype building in this study corresponds to 114 workers. Work across
496 multiple floors can take place simultaneously as long as the above constraints are met.

497 Lastly, utility disruption is also considered when estimating downtime for functional
498 recovery. Disruption to water, natural gas and electrical systems is considered. The time

499 required for achieving a 50% recovery of the system is assumed as 21, 42 and 3 days for
500 water, natural gas and electrical systems respectively. Acknowledging the difficulty in
501 performing accurate predictions of utility disruption, the REDi guidelines present a best
502 estimate of recovery based on an assessment of performance of these systems in past
503 earthquakes. In the present study, utility disruption does not control over other impeding
504 factors in the overall downtime assessment and therefore do not have a direct impact on the
505 downtime estimates. Equation 1 illustrates the overall downtime calculation by subdividing
506 delays into the following categories: utility disruption, impeding factors and repair work.

507
508
$$\text{Downtime} = \text{MAX} (\text{Utility Disruption}^*, \text{Impeding Factor Delays}) + \text{Repair Work}^{**} \quad (1)$$

509 ^{*} For Full recovery and Functional Recovery only

510 ^{**} Including delays associated with long-lead time components

511

512 *Strategies for Increased Resilience*

513 In order enhance the seismic performance of the archetype building, a reduction in transient
514 and residual deformations is required. This objective can be achieved by adding stiffness,
515 damping or a combination of these to the structure. Two conceptual structural retrofit
516 schemes are considered. The first scheme consists in the introduction of an elastic spine with
517 steel bracing in the building core. The introduction of an elastic spine is intended to reduce
518 transient and residual interstory drifts up the building height. This concept has been
519 implemented in a number of retrofit projects in Japan and has been explored in studies such
520 as Günay et al. (2009) by means of introducing a rocking wall. A second retrofit scheme
521 consists in the introduction of base isolation at ground level and is intended to significantly
522 reduce the seismic demands to the structure. This technique has been implemented in a
523 number of retrofit projects in Japan (Kani and Katsuta 2009).

524 In addition to structural retrofit strategies, schemes for enhanced non-structural performance
525 are also adopted in this study. These consist on employing non-structural components that are

526 more resilient to earthquake damage. For instance, the component fragility function for
527 standard partition walls is designated in Table 2 by fragility C1011.001a, which has a median
528 value of 0.2% interstory drift ratio for DS 1. The component fragility for the enhanced
529 partition wall is designated by fragility C101.001d, which has a median value of 1.7%
530 interstory drift ratio for DS 1. This illustrates that enhanced non-structural components can
531 withstand significantly larger deformations before reaching the same damage state. These
532 differences result in less damage to the components in the enhanced building performance
533 model versus those in the standard building performance model for the same demand
534 parameter. In the case of the partition walls, where standard components are characterized by
535 little deformation capacity and undergo damage at low drift ratios, enhanced partition walls
536 can enable a shift of up to 1.5% drift before the initiation of damage. This is achieved through
537 a simple sliding/frictional connection detail which isolates the partition from lateral
538 deformations while at the same time providing some resistance to in-plane and out-of-plane
539 inertia forces as described in Araya-Letelier and Miranda (2012). The impact of using
540 enhanced non-structural components is evaluated in all three structural schemes considered.
541 When baseline non-structural components are used, these are referred to as standard non-
542 structural components. When non-structural components that are more resilient to earthquake
543 damage are used, there are referred to as enhanced non-structural components.

544 In order to minimize downtime, a number of mitigation measures can be adopted. As
545 illustrated in Equation 1, downtime to achieve re-occupancy is attributed to impeding factors
546 and the time required to repair damaged structural and non-structural components. Downtime
547 to achieve functional recovery is attributed to these same factors, but additionally considers
548 utility disruption. The mitigation measures considered in this study in order to minimize
549 delays associated with impeding factors are illustrated in Table 4. For instance, delays
550 associated with post-earthquake inspection can be minimized by joining the City and County

551 of San Francisco's Building Occupancy Resumption Program (BORP) to pre-certify a private
552 post-earthquake inspection rather than waiting for a city appointed inspector. Similarly,
553 delays associated with engineering and contractor mobilization can be minimized by
554 arranging contractual agreements with engineers and contractors to guarantee their services
555 immediately after an earthquake. For instance, as illustrated in Table 4, if damage to
556 structural components hinders re-occupancy, expected delays associated with engineering
557 mobilization are 12 weeks. However, these delays can be reduced down to 4 weeks by having
558 an engineer on contract. Similarly, for the same level of structural damage, expected delays
559 associated with contractor mobilization are 40 weeks, but these can be reduced to 7 weeks by
560 having a pre-arranged contract with a general contractor. Similar measures can be put in
561 place to minimize other impeding factors.

562 *Modeling Uncertainty*

563 Since there are many factors that can affect performance, such as intensity of ground shaking,
564 building construction quality, building response or vulnerability of contents among others,
565 there is significant uncertainty in the predicted performance of the building. However, losses
566 can be expressed as a performance function, i.e. probability of losses of a specified amount or
567 smaller incurred as a result of an earthquake. This uncertainty can be accounted by means of
568 Monte Carlo simulation, where each realization represents one possible performance outcome
569 for the building considering a single combination of possible values of each variable
570 considered. The authors used PACT (FEMA 2012), which utilizes this methodology, for
571 conducting the loss estimates for the archetype building and five schemes for enhanced
572 performance including structural only enhancements, non-structural only enhancements and a
573 combination of these. Each building performance assessment consists of 1000 realizations.
574 Structural modeling uncertainty results from inaccuracies in component modeling, damping
575 and mass assumptions. These uncertainties are associated with the level of building

576 definition, as well as the quality and completeness of the analytical model (FEMA 2012).
577 Within PACT, these uncertainties are accounted for by defining a value of dispersion to the
578 building definition and a value of dispersion to the analytical model. These values of
579 dispersion are defined as superior, average or limited to reflect the overall modeling
580 uncertainty. Since documents defining the building design were confirmed by visual
581 observation, the authors selected average values of dispersion for construction quality
582 assurance (FEMA 2012). Similarly, since the model contained most elements that contribute
583 to the strength and stiffness as well as robust non-linear components over the range of the
584 deformation response, the authors selected average values of dispersion for the quality of the
585 analytical model. These values of dispersion are used to amplify the dispersion in the
586 structural demand parameters, as illustrated in Figure 7, which are used as input to the PACT
587 analysis.

588 Residual drifts are an important consideration when estimating losses. Typical building repair
589 fragility as a function of residual drifts is a lognormal distribution with a median value of 1%
590 residual drift ratio and a dispersion of 0.3. Residual drifts predicted by non-linear analysis are
591 highly sensitive to component modeling assumptions (FEMA 2012). Accurate statistical
592 simulation of residual drift requires the use of advanced component models, careful attention
593 to cyclic hysteretic response, and a large number of ground motion pairs. Therefore, residual
594 drifts were estimated as a function of peak transient response of the structure and the median
595 story drift ratio calculated at yield based on FEMA P-58 (2012) recommendations. For each
596 realization, PACT uses the maximum residual story drift together with the building repair
597 fragility to determine if the building is deemed irreparable. If irreparable, repair cost and
598 repair time are taken as the building replacement values. In order to assess the impact of
599 residual drifts in the loss assessments, results were calculated with and without consideration
600 of residual drifts.

601 **Loss and Downtime Assessment**

602 As illustrated in Table 5, expected losses for the archetype building are in the order of \$46M
603 (34% of building cost). These losses are associated with the structural response demand
604 parameters illustrated in Fig 7a. A structural only retrofit scheme, which consists of the
605 introduction of an elastic spine with steel bracing in the building core, enables a reduction in
606 expected losses by roughly 25% to \$34M (25% of building cost). The structural response
607 demand parameters associated with this retrofit scheme are illustrated in Fig 7b. An alternate
608 structural only retrofit scheme, which consists of the introduction base isolation at ground
609 level, enables a reduction in expected losses by roughly 80%, to \$9M (7% of building cost).
610 The structural response demand parameters associated with this retrofit scheme are illustrated
611 in Fig 7c. A non-structural only scheme, which consists of the introduction of components
612 that are more resilient to earthquake damage, enables a reduction in expected losses by
613 roughly 32%, to \$31M (23% of building cost). When these non-structural enhancements are
614 used in conjunction with the elastic spine structural retrofit scheme, a 56% reduction in
615 expected losses, to \$20M (15% of building cost) is attained. Lastly, when these non-structural
616 enhancements are used in conjunction with the base isolation structural retrofit scheme, a
617 92% reduction in expected losses, to \$4M (3% of building cost) is achieved. These results
618 explicitly consider the impact of residual drifts. If the impact of residual drifts is neglected, a
619 reduction in expected losses is observed as illustrated in Table 5. These results can also be
620 visualized in Fig 8 by fitting all 1,000 realizations in each performance assessment to a
621 lognormal distribution. Since the engineering demand parameters used as input to the
622 building performance model are in line with current code requirements, it is no surprise that
623 expected losses in new tall buildings are not drastically different than those of older tall
624 buildings. The expected losses for an archetype 40 story building in the Los Angeles area

625 designed per current buildings codes under an equivalent intensity level are 23% of building
626 cost (Shome et al. 2013).

627 Fig 9 illustrates the contribution of different building components to the total expected losses.
628 Building components are grouped into five main categories: egress, façade, MEP, office
629 fitouts and structure. The performance groups associated with each one of these categories is
630 shown in Tables 2. There are similarities in the distribution of building components
631 contributing to the losses between the archetype building and the elastic spine structural
632 retrofit scheme with either standard or resilient structural components. This can be attributed
633 to the similarity in the demand parameter distribution throughout the height for both schemes,
634 as shown in Fig 7. The distribution of building components contributing to the losses for the
635 base isolated scheme is distinct due to the unique distribution in demand parameters
636 throughout the building height when compared to the other structural schemes. The use of
637 resilient non-structural building components enables a significant reduction in losses
638 attributed to damage to the façade (up to 93% for the elastic spine scheme), office fitouts (up
639 to 94% for the base isolated scheme) and MEP components (up to 97% for the base isolated
640 scheme). Structural losses are largely due to damage to fracture prone pre-Northridge
641 moment connections (70% to 90% depending on the structural scheme). However, these
642 losses vary in absolute value from \$5M for the archetype building to \$2M for the base
643 isolated scheme. Absolute losses attributed to egress are a result of direct damage to
644 elevators, which require repair costs ranging from \$9M for the archetype building to \$0.5M
645 for the base isolated scheme.

646 The discrepancies in the results with and without consideration of residual drifts can be
647 observed in Fig 8 by the dispersion of the lognormal distributions. For the archetype building
648 with standard non-structural components, the dispersion is 0.44 when residual drifts are
649 neglected and 0.61 when residual drifts are considered. Similarly, for the elastic spine scheme

650 with standard non-structural components, the dispersion has a value of 0.51 when residual
651 drifts are neglected and 0.64 when considered. This increase in the dispersion is smaller than
652 that of the archetype building. Lastly, for the base isolated case, the dispersion remains
653 effectively constant at approximately 0.86. A similar trend is observed for the schemes
654 considered when enhanced non-structural components are used. These observations highlight
655 how as the schemes considered become more resilient, there is less variability throughout the
656 set of realizations. Even though consideration of residual drifts increase the dispersion in the
657 building performance functions, as illustrated in Fig 8, their consideration is critical in the
658 loss estimate methodology since a building may be deemed irreparable if large residual drifts
659 are present. Furthermore, residual drifts are an important consideration in judging the post-
660 earthquake safety of a building. Field manuals for post-earthquake safety evaluation, such as
661 ATC 20-1 (2005), indicate that when any story in a building has noticeable leaning the
662 building should be posted with an ‘Unsafe’ placard, which categorizes the building as unsafe
663 for occupancy or entry. The REDi downtime assessment methodology assumes that residual
664 drifts are small and therefore the building is repairable. Consideration of residual drifts on the
665 downtime estimate results presented in Table 6 would increase expected values because for
666 large residual drifts, where the building is deemed unreparable, total downtime is that of
667 complete re-design and re-construction. FEMA P-58 (2012) proposes 4 damage states
668 associated with residual drift: Damage State 1 (DS1) requires no structural realignment,
669 though repairs may be required for non-structural components; Damage State 2 (DS2)
670 requires realignment of the structural frame and related structural repairs; Damage State 3
671 (DS3) requires major structural realignment to restore margin of safety for lateral stability
672 though the level of repair may not be economically feasible; lastly, Damage State 4 (DS4)
673 implies that the structure is in danger of collapse from aftershocks. Fig 10 illustrates
674 probability distribution of residual drifts for the baseline building, elastic spine and base

675 isolated retrofit schemes against the abovementioned damage states. The expected residual
676 drift for the baseline building is 0.44%, consistent with DS2. The expected residual drift for
677 the elastic spine retrofit scheme is 0.23%, just beyond the threshold of DS1. The expected
678 residual drifts for the base isolated scheme is 0.07%, consistent with DS1 and well below the
679 maximum out-of-plumb tolerance permitted in new construction.

680 In order to provide a more direct measure of resilience, the downtime to achieve building re-
681 occupancy and functional recovery for the archetype building and retrofit schemes considered
682 is presented in Table 6. These results illustrate that while structural retrofits may enable
683 significant reductions in losses, as seen in Table 5, these measures alone do not ensure a
684 building is resilient. An illustration of the impact of using enhanced non-structural
685 components as well as mitigation measures to minimize delays associated with impeding
686 factors is illustrated in Fig 11, where a breakdown of the different downtime contributors as
687 well as disaggregation of the impeding factors for the archetype building is shown. For the
688 same structural scheme, it can be observed that using enhanced non-structural components
689 and adopting mitigation measures can have a significant impact on downtime. Downtime for
690 re-occupancy for all structural schemes with standard non-structural components is largely
691 driven by delays associated with building inspection, contractor mobilization and long leads
692 components that require replacement. In addition to these delays, which are equal for all
693 schemes, repair times range from 32 weeks for the baseline and elastic spine schemes down
694 to 12 weeks for the base isolation scheme. Downtime for functional recovery for structural
695 schemes with standard non-structural components vary: 87, 72 and 59 weeks for the baseline,
696 elastic spine and base isolation schemes respectively. Utility disruption does not control
697 overall downtime estimates for functional recovery because delays associated with impeding
698 factors exceed those associated with utility disruption (see Equation 1). While delays are
699 consistent with those for re-occupancy, repair times are as follows: 46, 31 and 18 weeks for

700 the baseline, elastic spine and base isolation schemes respectively. Repair times for re-
701 occupancy are consistent between the baseline scheme and the elastic spine because, while
702 the elastic spine scheme reduces damage and losses to certain components, it does not
703 prevent damage to those components that hinder re-occupancy. However, repair times for
704 functional recovery for the elastic spine scheme are significantly lower than for the baseline
705 scheme because lower residual drifts reduce damage to elevators. When enhanced non-
706 structural components are adopted in addition to measures to mitigate delays, downtime for
707 re-occupancy can be drastically reduced to 14 weeks for the baseline and elastic spine
708 schemes and a day or less for the base isolated scheme. Furthermore, downtime for functional
709 recovery can be reduced to 32 weeks for the baseline case, 20 weeks for the elastic spine
710 scheme and a day or less for the base isolation scheme.

711 As discussed earlier, there is a great deal of uncertainty in the prediction of losses and
712 downtime associated with the seismic performance of the building. In addition to the high
713 level of uncertainty, there are also a number of limitations associated with this work relating
714 to the development of the archetype building, the analytical model of the structure and the
715 building performance model. Even though the development of the archetype building is based
716 on an existing tall building database, a review of existing building drawings and discussions
717 with practicing engineers of the time, access to this data was limited and therefore the
718 archetype building is not representative of the entire existing tall building stock. Additionally,
719 while the analytical model attempts to account for all sources of strength and stiffness
720 contribution to the seismic response of the structure, additional studies (large number of
721 analyses with varying modeling assumptions) are required to assess the sensitivity of
722 modeling parameters in the overall structural response. As earlier explained, the variability in
723 structural response is incorporated into the loss estimation methodology through a modeling
724 dispersion. Limitations to the building performance model result from building component

725 quantity estimates, component fragility functions and the downtime estimate methodology.
726 Structural and non-structural quantity estimates are based on the Normative Quantity
727 Estimation Tool (FEMA 2012) as opposed to specific inventories of the existing tall
728 buildings that are representative of the archetype building. Component fragility functions
729 (fragility and consequence data) were not explicitly developed for the different building
730 components, but rather adopted from a fragility database developed as part of FEMA P-58
731 (2012) project. Lastly, downtime estimates are developed based on the REDi guidelines.
732 Accurate predictions of downtime are difficult to achieve due to the large uncertainty and
733 factors involved. However, the methodology follows a rational approach and enables a best
734 estimate of disruption to achieve certain recovery states after an earthquake. A more complete
735 evaluation should also consider performance under various hazard levels, recognizing that the
736 design level earthquake is simply an index to evaluate overall risk. Evaluation of a wider
737 range of intensities (return periods) would establish whether the performance expressed in
738 terms of losses and downtime at a design level earthquake is a realistic and reliable basis for
739 making decisions and would enable conducting a cost-benefit analysis of the different
740 schemes considered.

741 **Summary and Conclusions**

742 A seismic performance assessment of existing tall steel-framed buildings has been presented
743 for a case study city, San Francisco, where an archetype tall building is designed based on an
744 inventory of the existing tall building stock. In order to influence decision making,
745 performance is reported as the expected consequences in terms of direct economic losses and
746 downtime. A number of strategies including structural retrofits, non-structural enhancements
747 and mitigation measures are proposed in order to achieve increased resilience. Expected
748 direct economic losses for the archetype building are in the order of 34% of building cost and
749 the adoption of structural retrofit schemes, enhanced non-structural components and

750 mitigation measures to minimize impeding factors enable up to a 92% reduction in losses.
751 The adoption of non-structural enhancements can enable significant reduction in losses
752 associated with the performance of the façade, office fitouts and MEP components, though
753 overall loss reduction is maximized when adopting both structural and non-structural
754 enhancements. Downtime for re-occupancy and functional recovery of the archetype building
755 is estimated at 71 weeks and 87 weeks respectively. When mitigation measures to reduce
756 delays are used in conjunction with both structural and non-structural enhancements, minimal
757 downtime for both re-occupancy and functional recovery can be achieved. The impact of
758 residual drifts in seismic loss estimates for the archetype building and retrofit schemes under
759 consideration is quantified. Consideration of residual drifts in the loss assessment yields an
760 increase in expected losses as well as an increase in the dispersions of the resulting
761 performance functions. Furthermore, building performance is categorized as a function
762 expected residual drifts, which indicates that the archetype building requires structural
763 realignment of the frame under a design level earthquake, whereas the retrofit schemes
764 presented reduce damage to levels requiring very minor or no structural realignment.
765 Future work should consider the development of additional archetype buildings that enable
766 representation of a larger proportion of the building stock. Additionally, time based
767 assessments in conjunction with cost benefit analyses of the different enhancement schemes
768 should be studied in order to incentivize the adoption of these retrofit measures. The results
769 of these studies should target building owners and policy makers, who can adopt measures to
770 ensure that the resilience of existing tall buildings enables a successful recovery following a
771 major earthquake.

772 **Tables**

773 **Table 1.** Lateral resisting system section sizes per the 1973 UBC design.

Level Range	Wide Flange Beams			Box Columns		
	Exterior Short Span	Interior Short Span	Interior Long Span	Interior	Ext. Short EL. (x)	Ext. Long EL. (y)
Base to 10	W36x256	W36x282	W30x124	22x22" t=3"	26x26" t=3"	20x20" t=2.5"
11 to 20	W33x169	W36x194	W27x84	20x20" t=2"	26x26" t=2.5"	20x20" t=2"
21 to 30	W33x118	W33x169	W27x84	18x18" t=1"	24x24" t=1.5"	18x18" t=1"
30 to Roof	W24x62	W27x84	W24x76	18x18" t=0.75"	24x24" t=3"	18x18" t=0.75"

774

775 **Table 2.** Fragility numbers, category, quantities, units, demand parameter (DP), number of
 776 damage states (NDS), median (M), dispersion (D), mean repair cost (MRC) and mean repair
 777 time (MRT) for the first damage state (DS1) of each component in the standard building
 778 performance model.

779

Fragility Number	Category	Quantity	Unit	DP	NDS	DS1			
						M	D	MRC	MRT (days)
B1031.001	Structure	3096	1 EA	IDR	3	0.040	0.40	\$12,107	34.66
B1031.011c	Structure	26	1 EA	IDR	3	0.040	0.40	\$21,363	58.64
B1031.021b	Structure	112	1 EA	IDR	3	0.040	0.40	\$10,246	30.13
B1031.021c	Structure	226	1 EA	IDR	3	0.040	0.40	\$11,446	33.66
B1035.041	Structure	456	1 EA	IDR	5	0.017	0.40	\$11,980	31.95
B1035.042	Structure	318	1 EA	IDR	5	0.017	0.40	\$12,313	34.77
B1035.051	Structure	1552	1 EA	IDR	5	0.017	0.40	\$16,653	45.71
B1035.052	Structure	856	1 EA	IDR	5	0.017	0.40	\$16,653	44.41
B2011.201a (B2022.202)	Façade	533 (6933)	390 SF (30 SF)	IDR	2	0.005 (0.020)	0.50 (0.30)	\$17,160 (\$1,320)	184.60 (1.00)
C1011.001a (C1011.001d)	Fitout	365	100 LF	IDR	3	0.002 (0.017)	0.60	\$2,733	8.04 (1.61)
C3011.001a	Fitout	28	100 LF	IDR	1	0.002	0.60	\$2,829	9.00
C3027.001	Fitout	2736	100 SF	A	1	0.500	0.50	\$121	0.43
C3032.001b	Fitout	547	600 SF	A	3	0.550	0.40	\$921	3.03
C3034.001	Fitout	6192	1 EA	A	1	0.600	0.40	\$483	1.51
E2022.023	Fitout	2554	1 EA	A	1	0.400	0.50	\$1,000	0.00
D2021.011a (D2021.014a)	MEP	6	1000 LF	A	2	1.500 (2.250)	0.40 (0.50)	\$348	1.02
D2022.011a	MEP	37	1000 LF	A	2	0.550	0.50	\$279	1.00
D2022.011b	MEP	37	1000 LF	A	2	1.200	0.50	\$383	1.00
D2022.021a	MEP	14	1000 LF	A	2	1.500	0.50	\$348	1.00
D2031.021a	MEP	24	1000 LF	A	1	2.250	0.50	\$3,167	9.31
D2031.021b	MEP	24	1000 LF	A	2	1.200	0.50	\$423	1.25
D3041.011a	MEP	31	1000 LF	A	2	1.500	0.40	\$681	2.00
D3041.012a	MEP	8	1000 LF	A	2	1.500	0.40	\$996	2.29
D3041.031a	MEP	372	10 EA	A	1	1.300	0.40	\$2,833	10.00
D3041.041a	MEP	289	10 EA	A	1	1.900	0.40	\$14,796	41.49
D4011.021a	MEP	83	1000 LF	A	2	1.100	0.40	\$348	1.05
D4011.031a	MEP	37	100 EA	A	2	0.750	0.40	\$526	1.25
D5012.021a	MEP	43	1 EA	A	1	1.280	0.40	\$9,707	9.25
D3031.011c	MEP	2	500 TN	A	1	0.200	0.40	\$263,967	248.19
D3031.021c	MEP	2	500 TN	A	1	0.500	0.40	\$134,657	126.74
D3052.011d	MEP	13	30000 CF	A	2	0.250	0.40	\$2,066	6.48
D5012.013a	MEP	17	1 EA	A	1	0.730	0.45	\$4,167	10.62
C2011.001b (C2011.001a)	Egress	43	1 EA	IDR	3	0.005 (0.010)	0.60	\$394	1.08
D1014.011	Egress	12	1 EA	A	4	0.390	0.45	\$1,333	3.90
D1014.014	Egress	12	1 EA	Res-IDR	1	0.002	0.30	\$1,200,000	180.00

Table 3. Labor allocation parameters for repair time estimates. Adapted from REDi.

Component Category	Number of Workers	Maximum Number of Workers
Structure	1 per 500 ft ²	20
Façade	1 per 1000 ft ²	45
Office Fitouts	1 per 1000 ft ²	45
Egress	2 per Damaged Unit	27
MEP	3 per Damaged Unit	18

784
785

Table 4. Mitigation measures to minimize delays associated with impeding factors. Adapted from REDi.

Impeding Factor	Mitigation Measure	Other Conditions	Mean	Dispersion
Post-Earthquake Inspection	None	-	5 days	0.54
	BORP Program	-	1 day	0.54
Engineering Mobilization	None	Damage to structural components does not hinder Full Recovery	6 weeks	0.40
		Damage to structural components hinders Re-occupancy	12 weeks	0.40
		Complete re-design required	50 weeks	0.30
	Engineer on Contract	Damage to structural components does not hinder Full Recovery	2 weeks	0.30
		Damage to structural components hinders Re-occupancy	4 weeks	0.50
		Complete re-design required	42 weeks	0.50
Contractor Mobilization	None	Damage to structural components does not hinder Full Recovery	28 weeks	0.30
		Damage to structural components hinders Re-occupancy	40 weeks	0.30
	General Contractor on Contract	Damage to structural components does not hinder Full Recovery	3 weeks	0.70
		Damage to structural components hinders Re-occupancy	7 weeks	0.40
Financing	None	Private Loans	15 weeks	0.70
	Pre-arranged Credit	-	1 week	0.50
Permitting	None	Damage to structural components does not hinder Full Recovery	1 week	0.90
	Minimize Structural Damage	Damage to structural components hinders Re-occupancy	8 weeks	0.30

786

787

788 **Table 5.** Expected loss estimates for the baseline building and enhanced performance
 789 schemes with and without consideration of residual drifts.

Residual Drift Considered		Non-structural		Residual Drift Neglected		Non-structural	
		Standard	Enhanced			Standard	Enhanced
Structural	Archetype (Baseline)	\$46M (34%)	\$31M (23%)	Structural	Archetype (Baseline)	\$35M (25%)	\$19M (14%)
	Elastic Spine	\$34M (25%)	\$20M (15%)		Elastic Spine	\$29M (21%)	\$13M (10%)
	Base Isolation	\$9M (7%)	\$4M (3%)		Base Isolation	\$9M (7%)	\$4M (3%)

790

791 **Table 6.** Downtime estimates for the baseline building and enhanced performance schemes
 792 for re-occupancy and functional recovery.

Re-occupancy		Non-structural		Functional Recovery		Non-structural	
		Standard	Enhanced			Standard	Enhanced
Structural	Archetype (Baseline)	72 weeks	14 weeks	Structural	Archetype (Baseline)	87 weeks	32 weeks
	Elastic Spine	72 weeks	14 weeks		Elastic Spine	72 weeks	20 weeks
	Base Isolation	53 weeks	1 day		Base Isolation	59 weeks	1 day

793

794 **Acknowledgments**

795 The authors would like to acknowledge the SEAONC Tall Buildings Committee for their
 796 effort in developing the existing tall building database for San Francisco. We would like to
 797 thank Jack Baker and Jongwon Lee for their guidance in the seismic hazard and ground
 798 motion selection work. We would like to thank Sean Merrifield and Jenni Tipler for their
 799 support in the development of the PACT analysis model and Eduardo Miranda for his
 800 guidance on the overall loss assessment, particularly with regards to residual drift
 801 considerations. We would like to thank Laurence Kornfield for providing insight on how to
 802 maximize the impact of this work on future policy in San Francisco. We would also like to
 803 thank Arup for providing research funds to conduct this work. Lastly, we would also like to
 804 thank Tiziana Rossetto for enabling Carlos Molina Hutt to temporarily relocate to San
 805 Francisco to work on this research.

806

807 **References**

- 808 Almufti, I., Motamed , R., Grant, D. and Willford, M. (2013). “Incorporation of velocity
809 pulses in design ground motions for response history analysis using a probabilistic
810 framework.” *Earthquake Spectra*, accepted.
811
- 812 Almufti, I. and Willford, M. (2013). “Resilience-based Earthquake Design Initiative (REDi)
813 for the Next Generation of Buildings.” Arup,
814 <http://publications.arup.com/Publications/R/REDi_Rating_System.aspx> (Sept. 1, 2014).
815
- 816 Araya-Letelier, G. and Miranda E. (2012). “Novel Sliding/Frictional Connections for
817 Improved Seismic Performance of Gypsum Wallboard Partitions.” *Proc., 15th World
818 Conference of Earthquake Engineering*, Lisbon, Portugal.
819
- 820 ASCE (2010). “Minimum design loads for buildings and other structures.” ASCE/SEI 7-10,
821 American Society of Civil Engineers, Reston, VA.
822
- 823 ATC (2005). “Field manual: postearthquake safety evaluation of buildings (second edition)”.
824 ATC-20-1, Applied Technology Council, Redwood City, California.
825
- 826 Baker, J. (2011). “Conditional Mean Spectrum: Tool for ground motion selection.” *Journal of
827 Structural Engineering*, 137(3), 322–331
828
- 829 Baker, J. and Jayaram, N. (2008). “Correlations of spectral acceleration values from NGA
830 ground motion models.” *Earthquake Spectra*, 23(1), 299-317.
831
- 832 Bonowitz, D. (2011). “Resilience Criteria for Seismic Evaluation of Existing Buildings.” A
833 2008 Special Projects Initiative Report to Structural Engineers Association of Northern
834 California, San Francisco, California.
835
- 836 Bruneau, M., Chang, S., Eguchi, T., Lee, G., O’Rourke, T., Reinhorn, A., Shinozuka, M.,
837 Tierney, K., Wallace, W. and Winterfeldt, D. (2003). “A Framework to Quantitatively Assess
838 and Enhance the Seismic Resilience of Communities.” *Earthquake Spectra*, 19(4). 733–752.
839
- 840 Bruneau, M. and Mahin, S. (1990). “Ultimate behavior of heavy steel section welded splices
841 and design implications.” *Journal of Structural Engineering*, 116(8).
842
- 843 Bruneau, M. and Reinhorn, A. M. (2006). “Overview of the Resilience Concept.” *Proc., 8th
844 U.S. National Conference on Earthquake Engineering*, San Francisco, CA.
845
- 846 Bruneau, M. and Reinhorn, A. M. (2007). “Exploring the concept of seismic resilience for
847 acute care facilities.” *Earthquake Spectra*, 23(1), 41-62.
848
- 849 CERC (2012). “Christchurch, the city and approach to this inquiry.” Canterbury Earthquakes
850 Royal Commission, Final Report, Volume 5, Canterbury, New Zealand.
851
- 852 Cimellaro, G. P., Reinhorn, A. M. and Bruneau, M. (2006). “Quantification of Seismic
853 Resilience.” *Proc., 8th U.S. National Conference on Earthquake Engineering*, San Francisco,
854 CA.
855

856 Cimellaro, G. P., Reinhorn, A. M. and Bruneau, M. (2010). "Framework for analytical
857 quantification of disaster resilience." *Engineering Structures*, 32 (2010) 3639-3649.
858

859 Cimellaro, G. P., Villa, O. and Bruneau, M. (2014). "Resilience-Based Design of Natural Gas
860 Distribution Networks." *ASCE Journal of Infrastructure Systems*, 05014005(14).
861

862 Comerio, M. (2006). "Estimating Downtime in Loss Modeling." *Earthquake Spectra*, 22(2),
863 349-365.
864

865 FEMA (2000). "Recommended postearthquake evaluation and repair criteria for welded steel
866 moment-frame buildings. Program to reduce the hazards of steel moment frame structures."
867 FEMA 352, Federal Emergency Management Agency, Washington, D.C.
868

869 FEMA (2006). "Next generation performance based seismic design guidelines. Program plan
870 for new and existing buildings." FEMA 445, Prepared by the Applied Technology Council
871 for the Federal Emergency Management Agency, Washington, D.C.
872

873 FEMA (2012). "Seismic performance assessment of buildings." FEMA P-58, Prepared by the
874 Applied Technology Council for the Federal Emergency Management Agency, Washington,
875 D.C.
876

877 Günay S., Korolyk M., Mar D., Mosalam K.M. and Rodgers J. (2009). "Infill walls as a spine
878 to enhance the seismic performance of non-ductile reinforced concrete frames." *Proc.,
879 Applied Technology Council and the Structural Engineering Institute 2009 Conference on
880 Improving the Seismic, Performance of Existing Buildings and Other Structures*, San
881 Francisco, CA.
882

883 Gupta A. and Krawinkler H. (1999). "Seismic Demands for Performance Evaluation of Steel
884 Moment Resisting Frame Structures." Dept. of Civil and Environmental Engineering,
885 Stanford University. Report No. 132, Stanford, California.
886

887 IBC (2012). "2012 International Building Code." IBC 2012, International Code Council,
888 INC.
889

890 Jayaram, N. and Shome N. (2012). "A Statistical Analysis of the Response of Tall Buildings
891 to Recorded and Simulated Ground Motions." *Proc., 15th World Conference of Earthquake
892 Engineering*, Lisbon, Portugal.
893

894 Kani, N. and Katsuta, S. (2009). "Seismic Isolation Retrofit for Existing Buildings in Japan."
895 *Proc., Applied Technology Council and the Structural Engineering Institute 2009
896 Conference on Improving the Seismic, Performance of Existing Buildings and Other
897 Structures*, San Francisco, CA.
898

899 Khater, M., Scawthron, C. and Johnson, J. (2002). "Loss Estimation." *Earthquake
900 Engineering Handbook*, Chapter 31, CRC Press, Boca Raton, Florida, USA.
901

902 Krawinkler, H. and Miranda, E. (2004). Performance-Based Earthquake Engineering. In:
903 Bozorgnia Y. and Bertero V., *Earthquake Engineering: From Engineering Seismology to
904 Performance-Based Engineering*, CRC Press, Chapter 9.
905

906 Kurata, M., Suita, K. and Nakashima, M. (2005). “Test on large cyclic deformation of steel
907 tube columns having fixed column bases.”, *Journal of Structural and Construction*
908 *Engineering*, 598,149-154.
909

910 Lignos, D. and Krawinkler, H. (2010). “A steel database for component deterioration of
911 tubular hollow square steel columns under varying axial load for collapse assessment of steel
912 structures under earthquakes”. *Joint Conference Proceedings: 7th International Conference on*
913 *Urban Earthquake Engineering & 5th International Conference on Earthquake Engineering*,
914 Tokyo Institute of Technology, Tokyo, Japan.
915

916 LS-DYNA (2013). Livermore Software Technology Corporation (LSTC) Version 971.
917

918 Maison, F. and Bonowitz, D. (1999). “How safe are pre-Northridge WSMFs? A case study of
919 the SAC Los Angeles nine-story building.” *Earthquake Spectra*, 15(4).
920

921 Miranda, E. and Aslani, H. (2003). “Probabilistic Response Assessment for Building-Specific
922 Loss Estimation.” Pacific Earthquake Engineering Research Center, Report No. 2003/03,
923 College of Engineering, University of California, Berkeley.
924

925 Moehle, J. and Deierlein, G. (2004). “A framework methodology for performance-based
926 earthquake engineering.” *Proc., 13th World Conference of Earthquake Engineering*,
927 Vancouver, B.C., Canada
928

929 Muto, M. and Krishnan, S. (2011). “Hope for the Best, Prepare for the Worst: Response of
930 Tall Steel Buildings to the ShakeOut Scenario Earthquake.” *Earthquake Spectra*, 27(2).
931

932 PEER (2010a). “Tall buildings initiative: guidelines for performance-based seismic design of
933 tall buildings.” Pacific Earthquake Engineering Research Center, Report No. 2010/05,
934 College of Engineering, University of California, Berkeley.
935

936 PEER (2010b). “Modeling and acceptance criteria for seismic design and analysis of tall
937 buildings.” Pacific Earthquake Engineering Research Center, Report No. 2010/111 also
938 published as PEER/ATC-72-1, College of Engineering, University of California, Berkeley,
939 CA.
940

941 Porter, K. and Kiremidjian, A .S. (2001). “Assembly-Based Vulnerability of Buildings and Its
942 Uses in Seismic Performance Evaluation and Risk Management Decision-Making” Dept. of
943 Civil and Environmental Engineering, Stanford University. Report No. 139, Stanford,
944 California.
945

946 SAC (2000). “Performance prediction and evaluation of steel special moment frames for
947 seismic loads.” SAC Steel Project, Report No. SAC/BD-00/25, Richmond, CA.
948

949 SEAOC (1973) “Recommended lateral force requirements and commentary.” Seismology
950 Committee, Structural Engineers Association of California, Sacramento, CA.
951

952 Shahi, S. K. and Baker, J.W. (2011). “An empirically calibrated framework for including the
953 effects of near-fault directivity in probabilistic seismic hazard analysis.” *Bulletin of the*
954 *Seismological Society of America*, 101(2), 742–755.
955

956 Shome N., Jayaram, N. and Rahnema, M. (2013). “Development of Earthquake Vulnerability
957 Functions for Tall Buildings.” *Proc., 11th International Conference on Structural Safety and*
958 *Reliability*, New York, USA.

959

960 SISMIC (2012). Oasys Sismic: Probabilistic Seismic Hazard Program, Version 9.2.0.10b,
961 Arup.

962

963 SPUR (2012). “Safe Enough to Stay.” San Francisco Planning and Urban Research
964 Association, <<http://www.spur.org/publications/spur-report/2012-02-01/safe-enough-stay> >
965 (Sept. 1, 2014).

966

967 UBC (1973). “Uniform building code 1973 edition.” UBC 73, International Conference of
968 Building Officials, Whittier, CA.

969

970 Wang, C. and Blackmore, J. (2009). “Resilience Concepts for Water Resource Systems.”
971 *ASCE Journal of Water Resources Planning and Management*, 116(8).

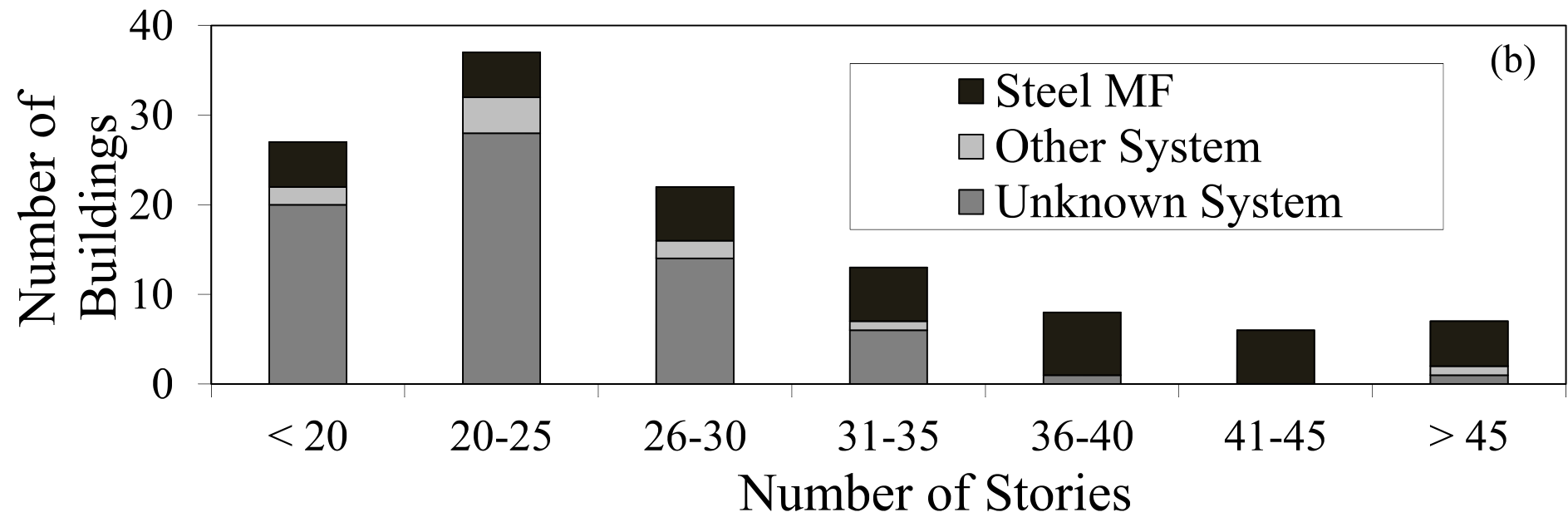
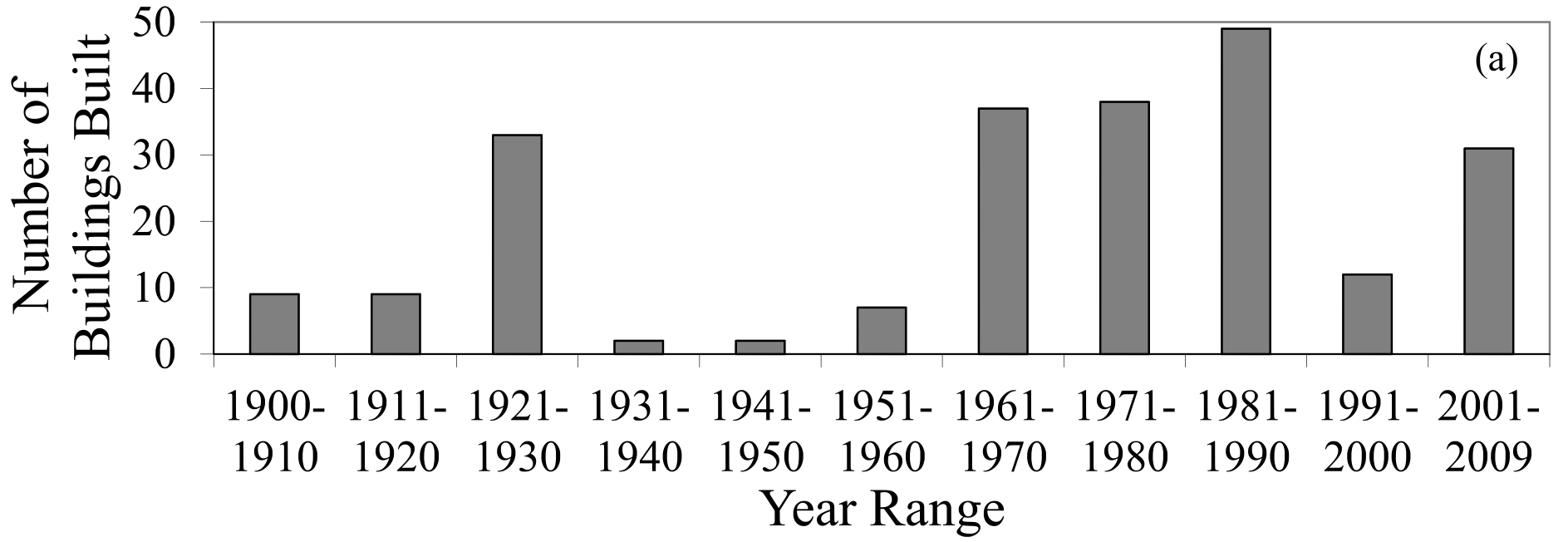
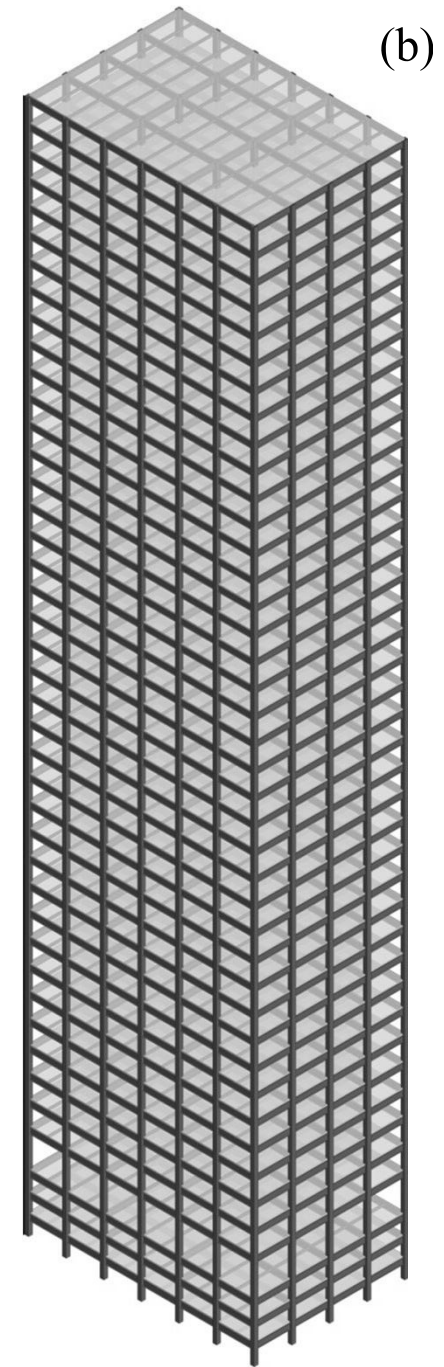
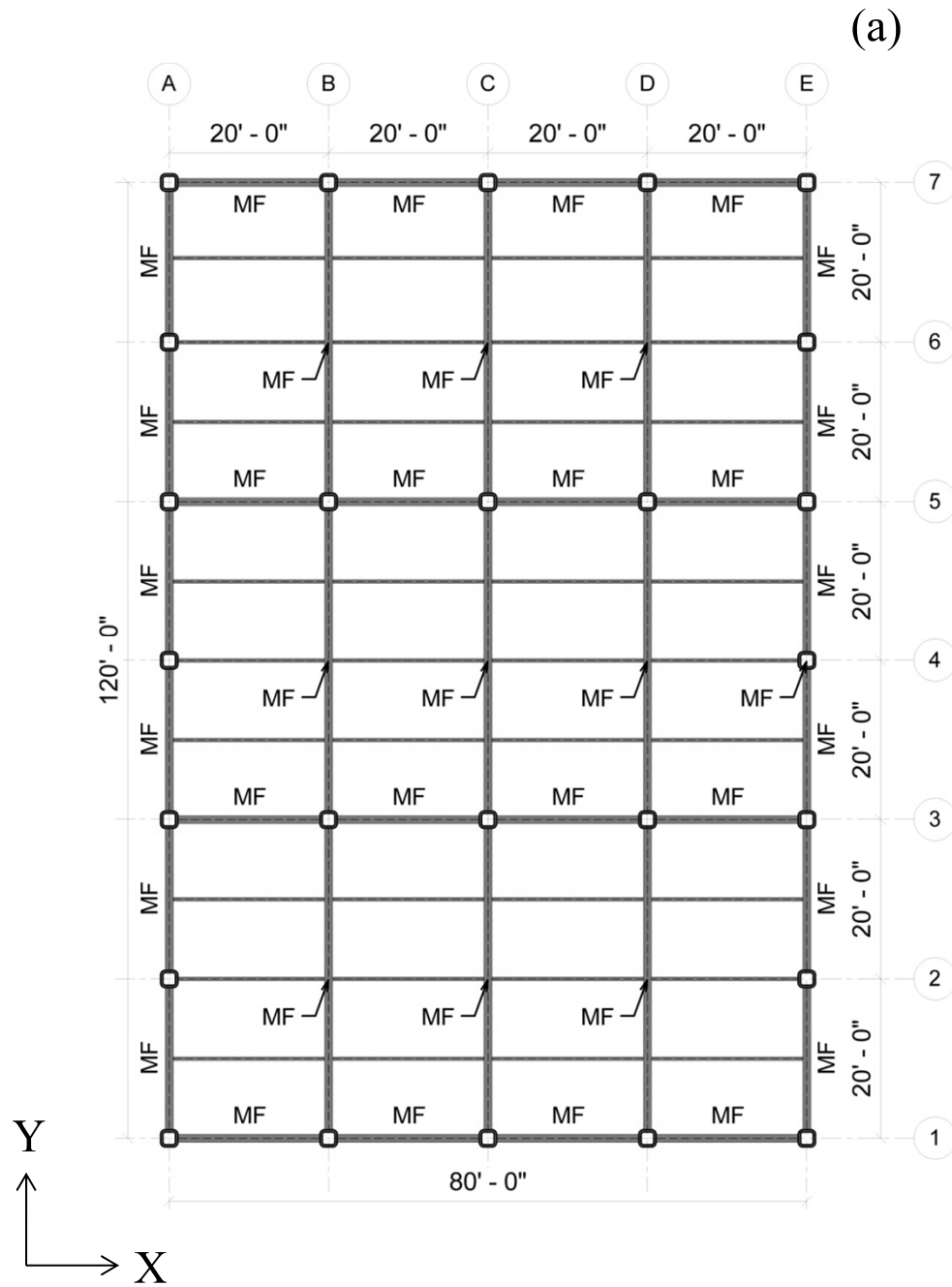
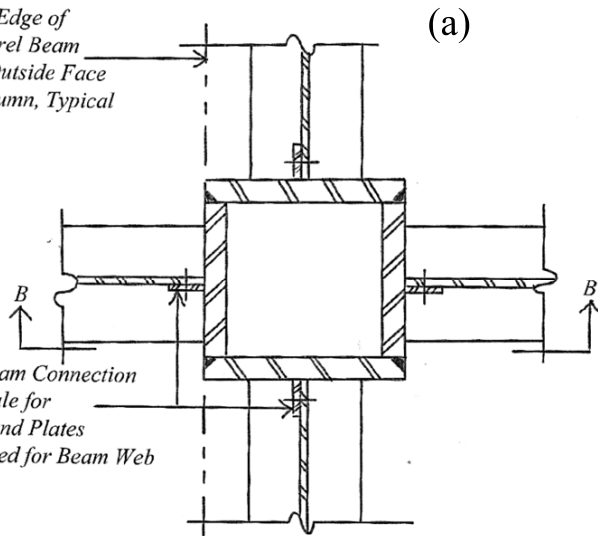


Figure 02
[Click here to download Figure: Figure_02.pdf](#)



Align Edge of Spandrel Beam with Outside Face of Column, Typical

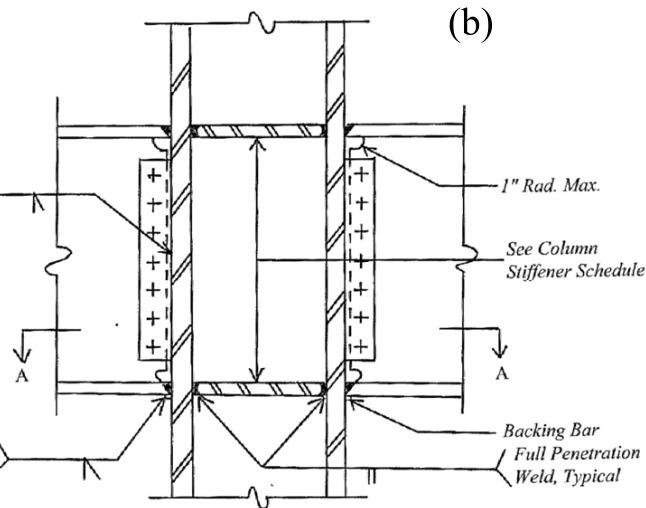
See Beam Connection Schedule for Bolts and Plates Required for Beam Web



(a)

See Beam Connection Schedule

Full Penetration Weld, Typical



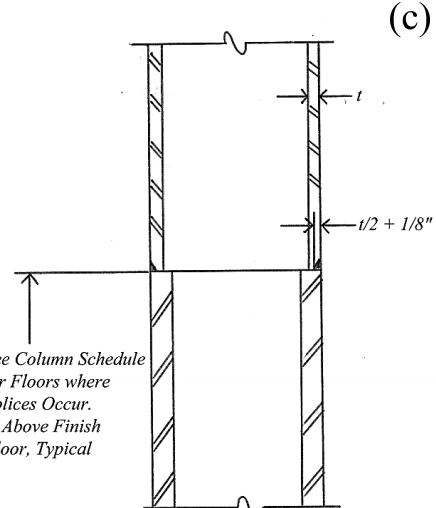
(b)

1" Rad. Max.

See Column Stiffener Schedule

Backing Bar Full Penetration Weld, Typical

See Column Schedule for Floors where Splices Occur. 4' Above Finish Floor, Typical



(c)

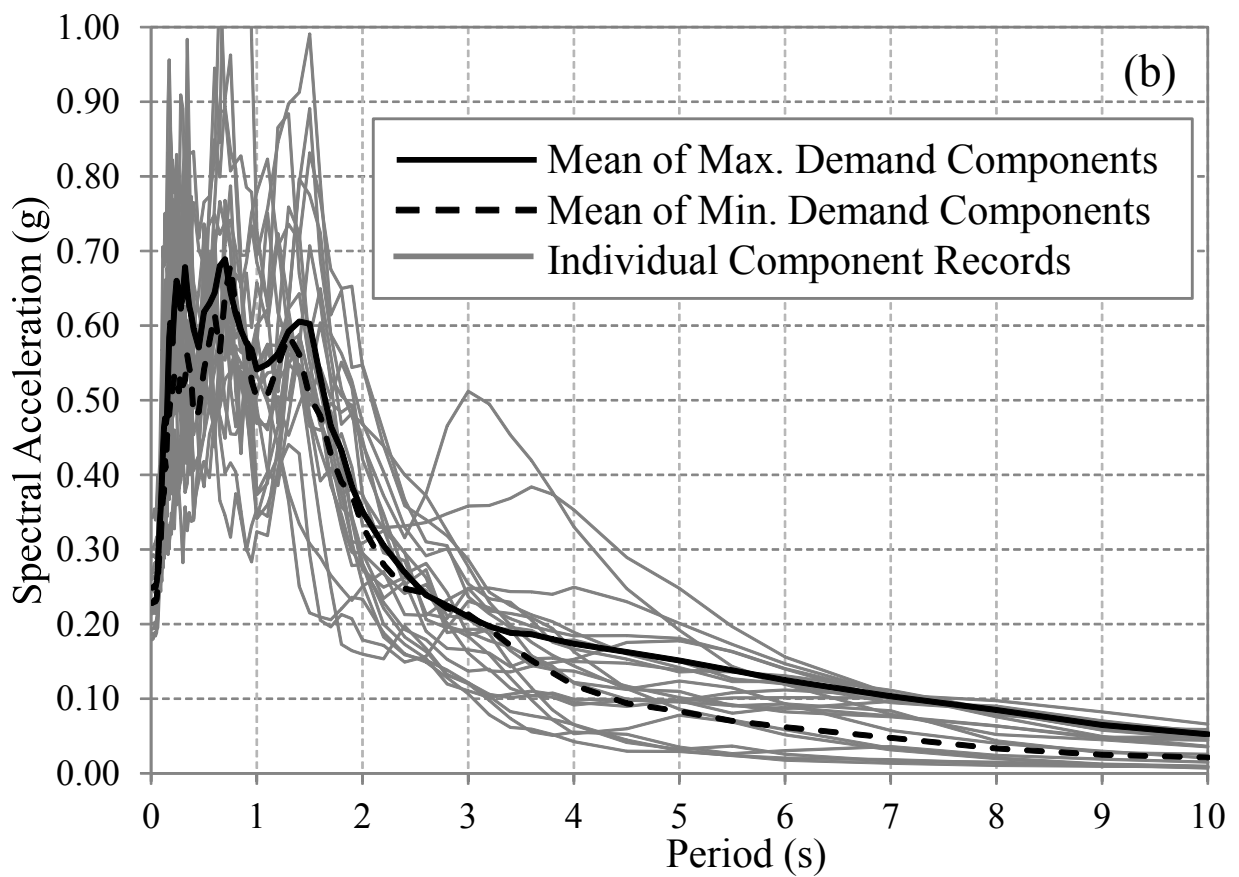
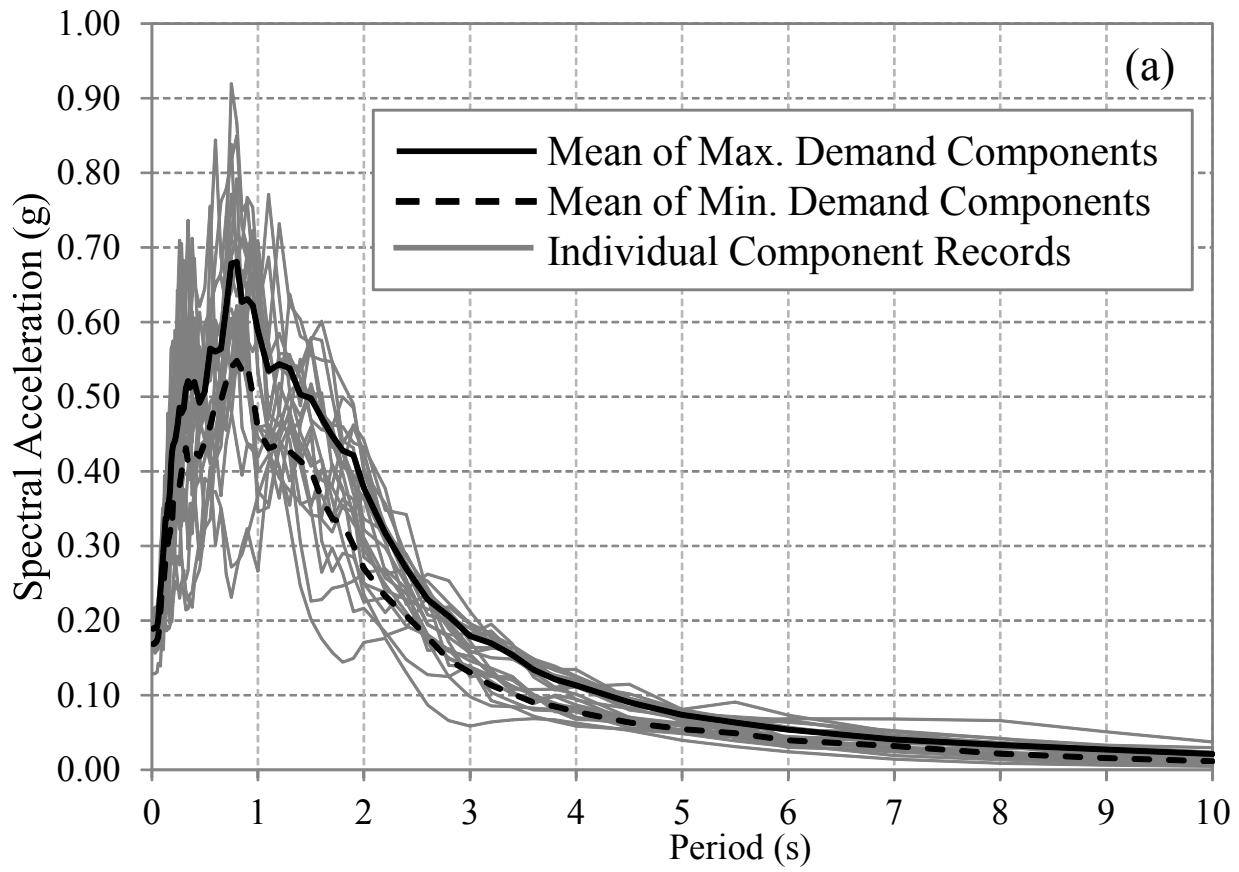


Figure 05
[Click here to download Figure: Figure_05.pdf](#)

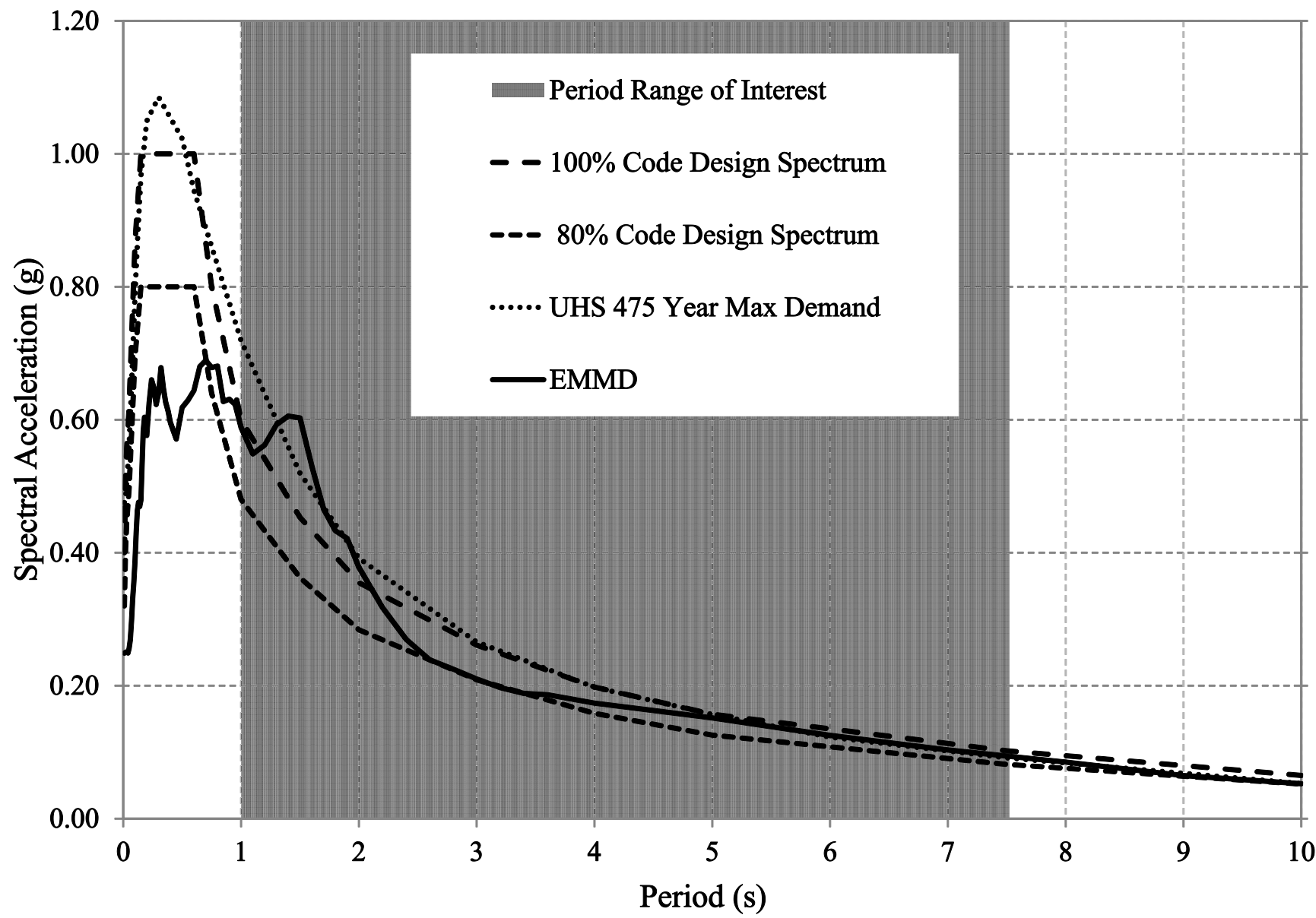
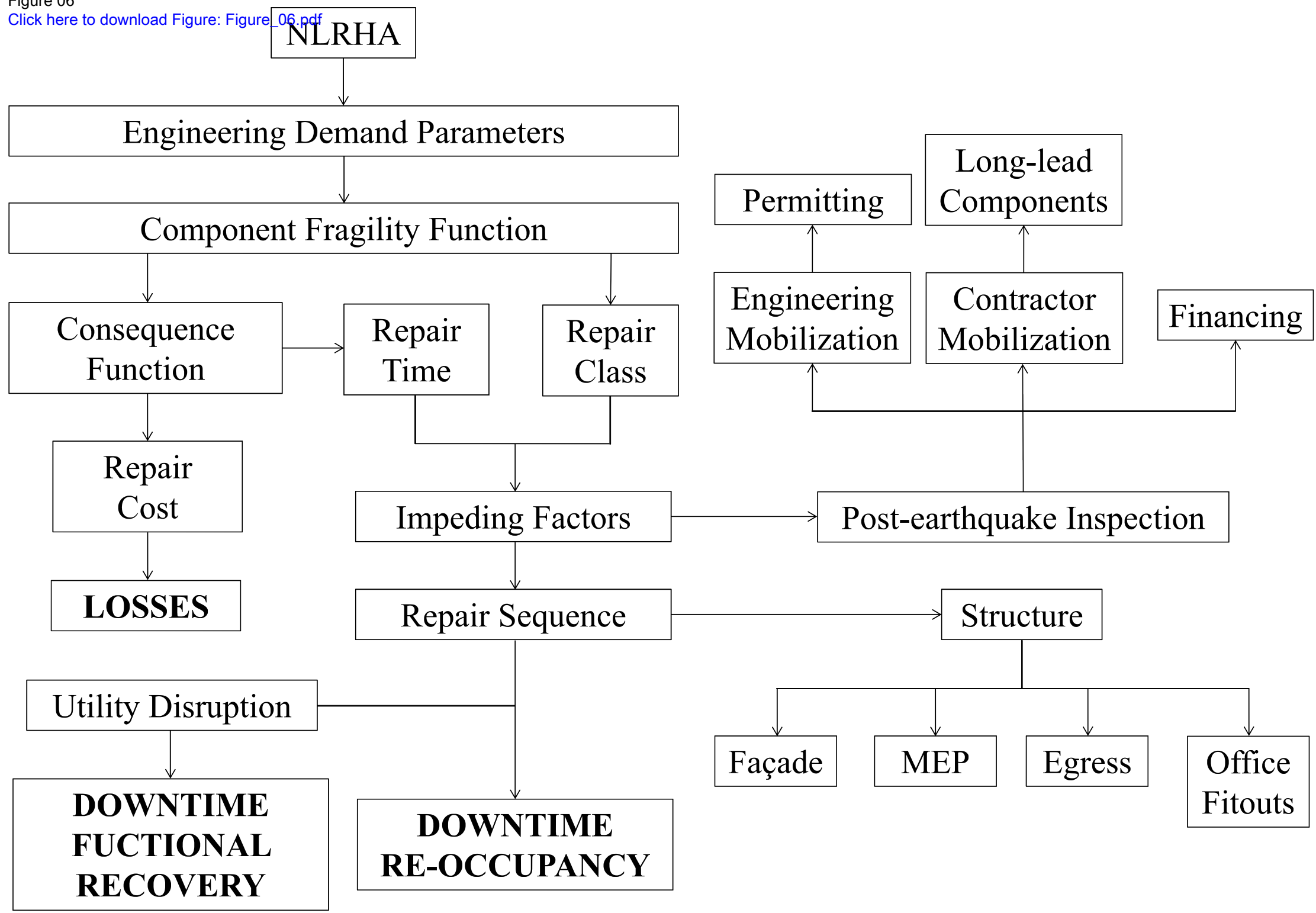


Figure 06
[Click here to download Figure: Figure_06.pdf](#)



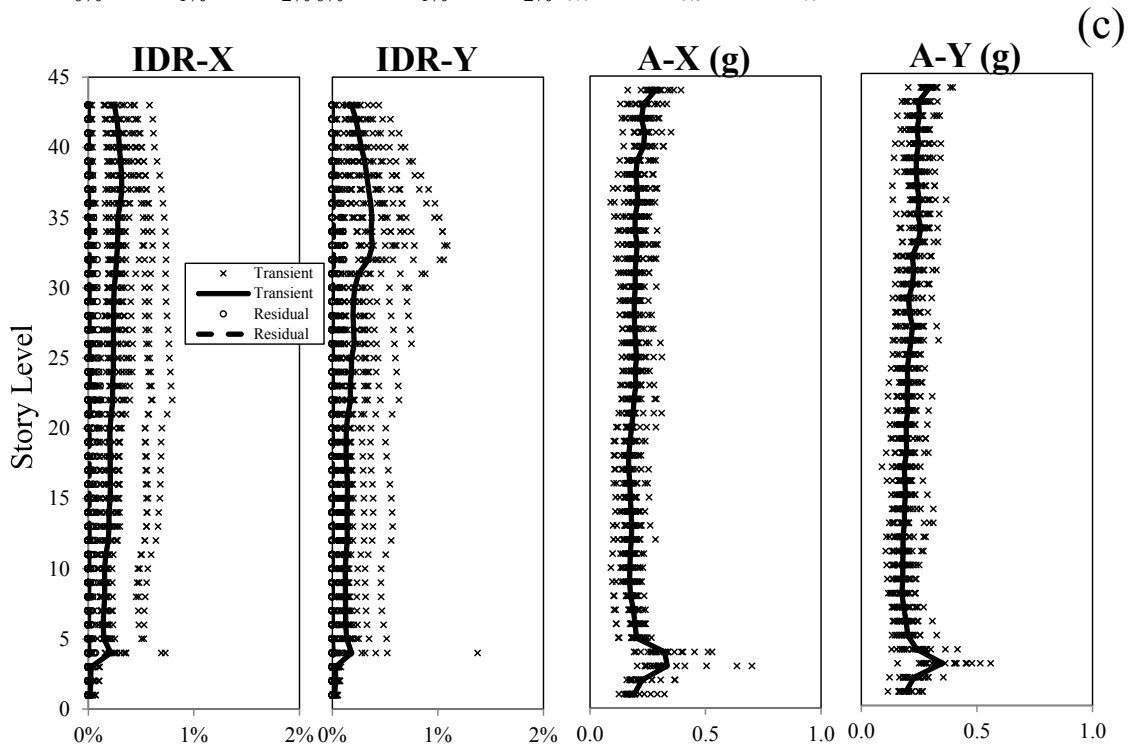
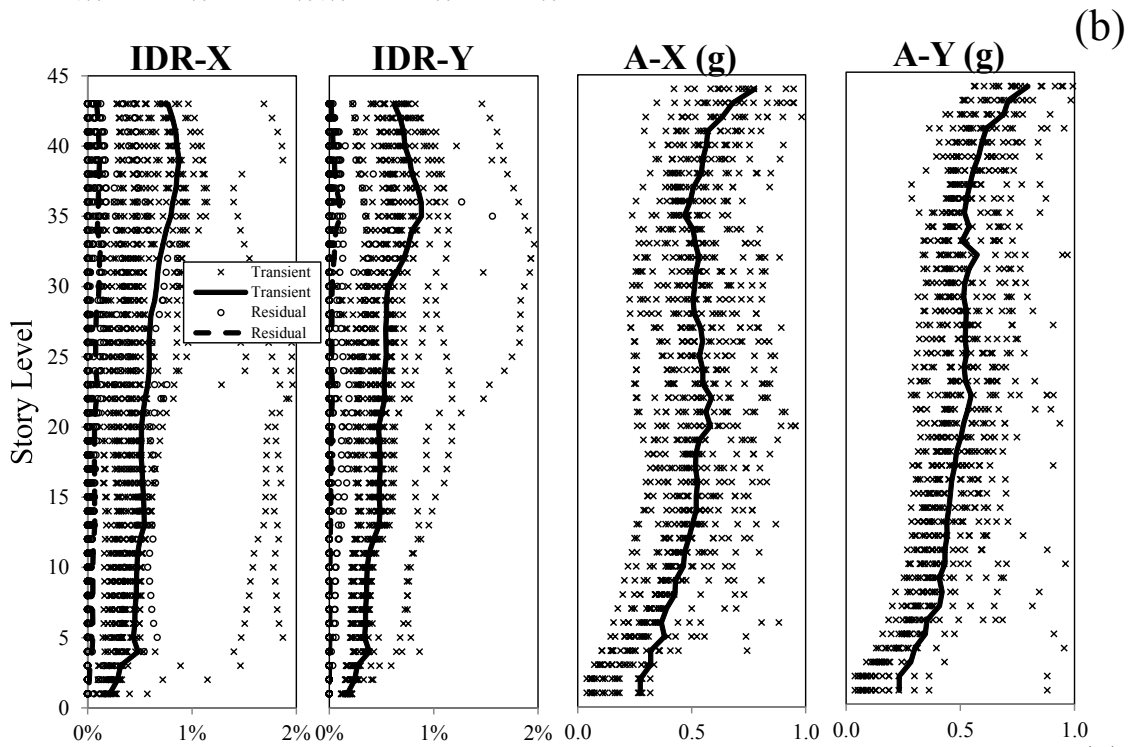
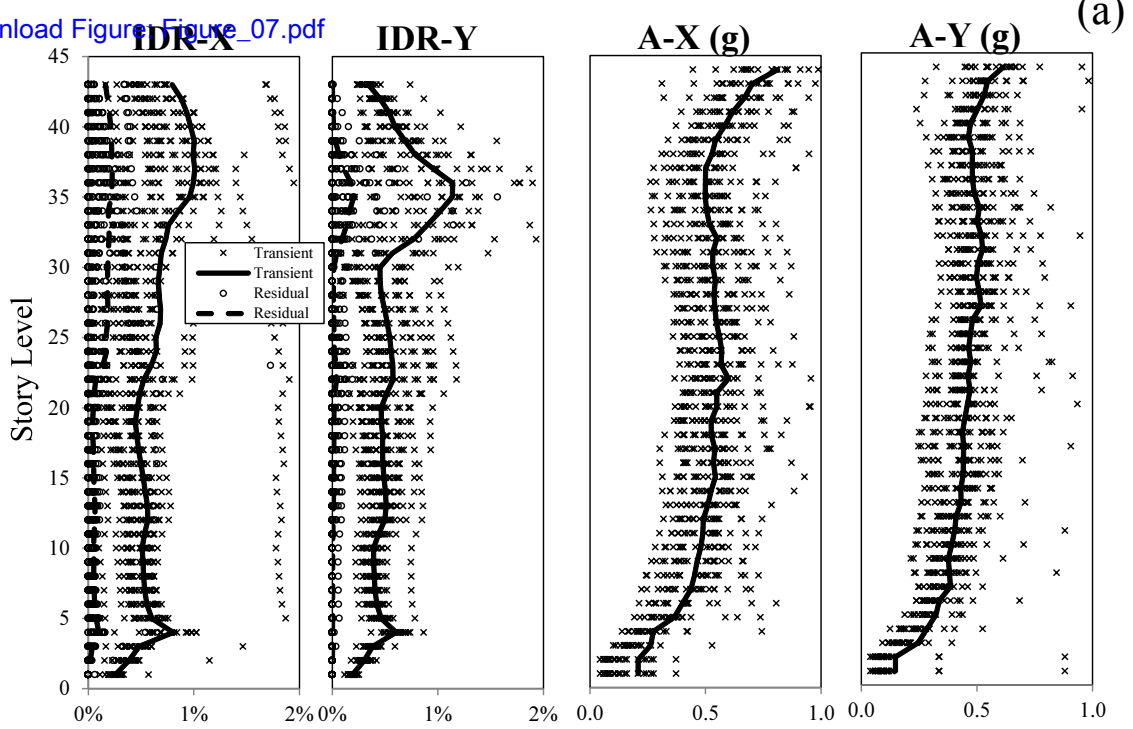
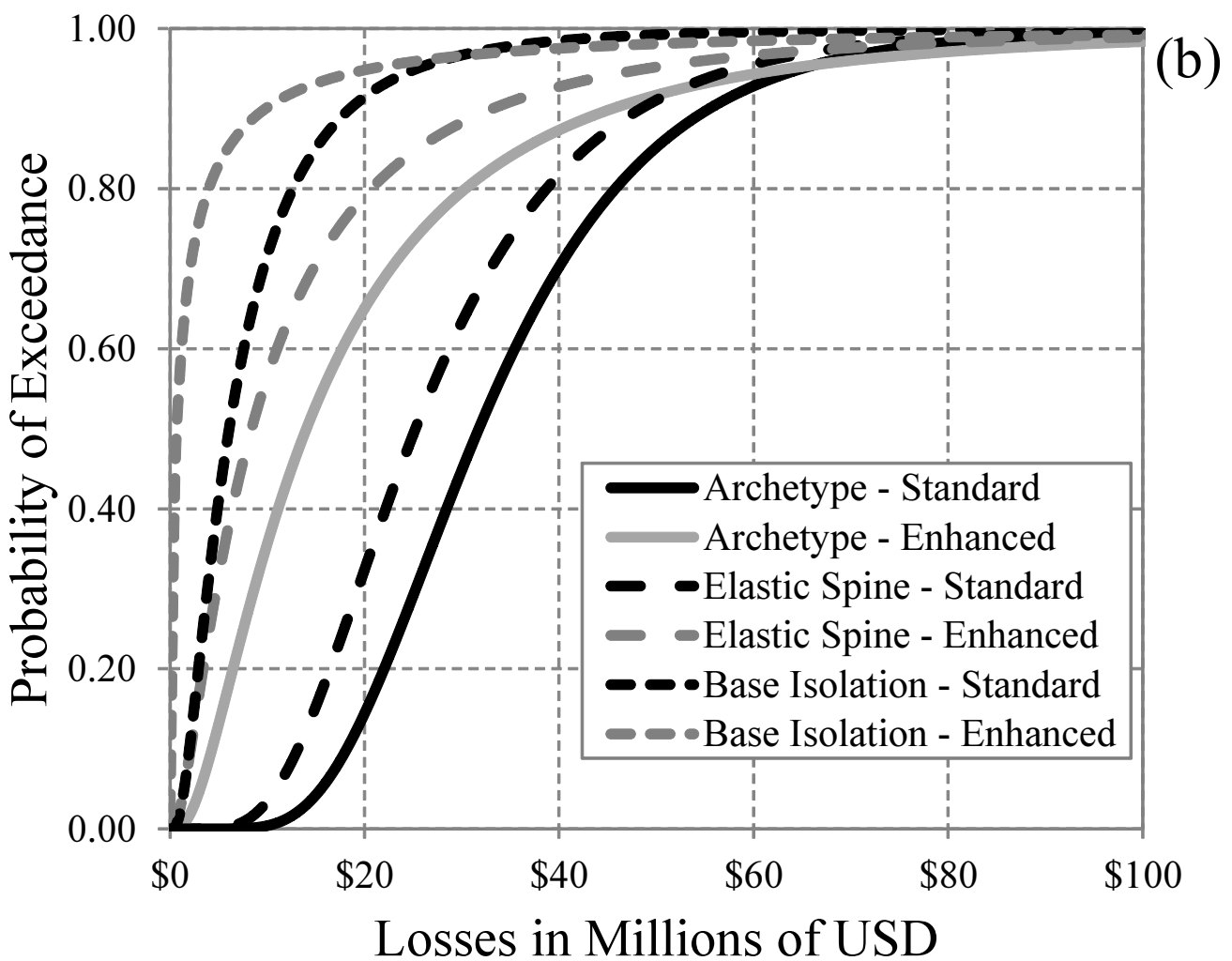
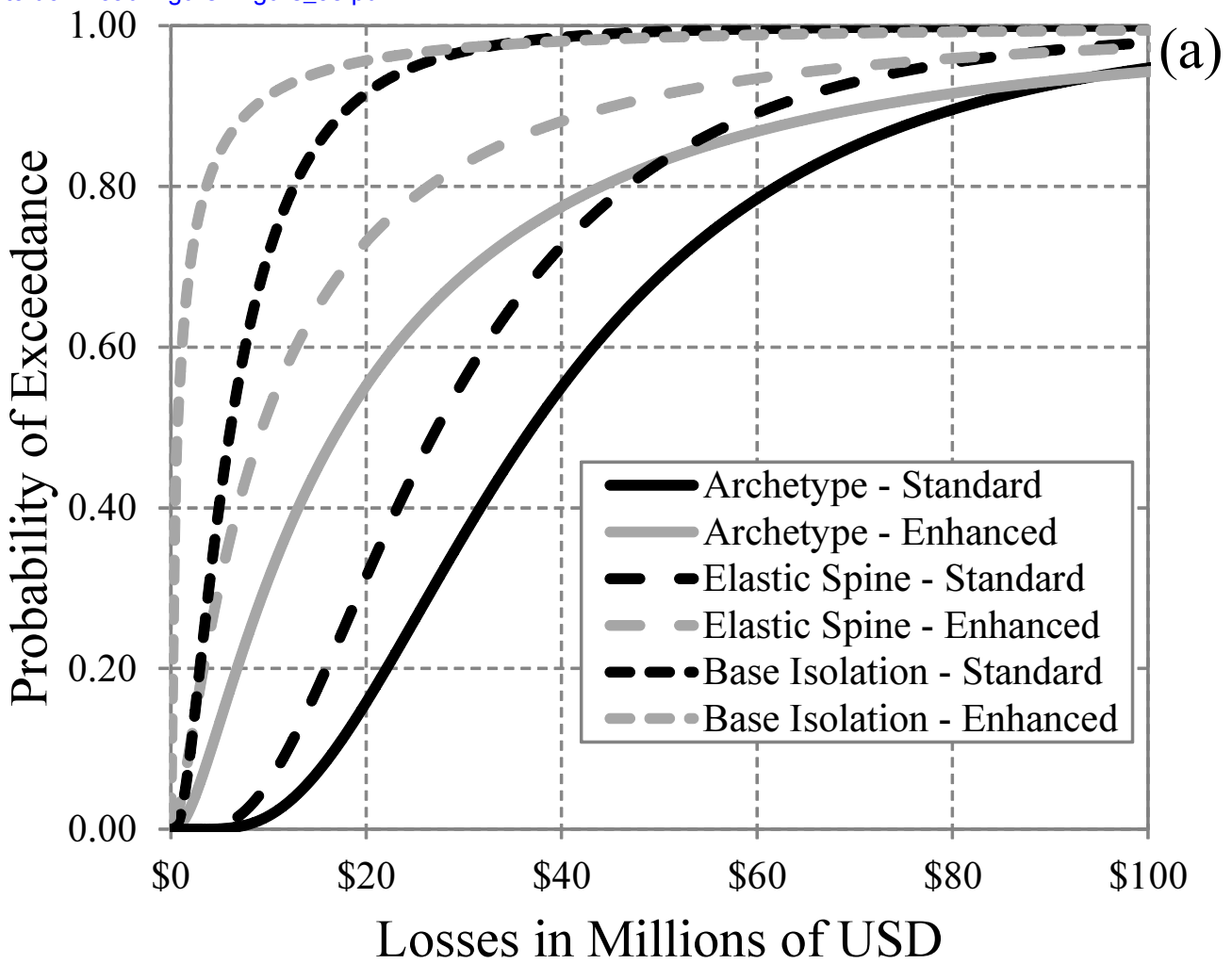


Figure 08

[Click here to download Figure: Figure_08.pdf](#)



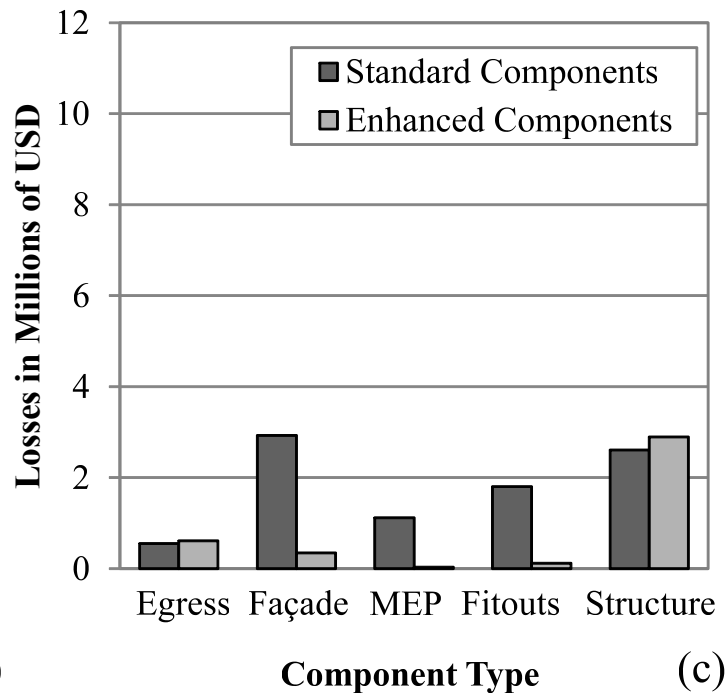
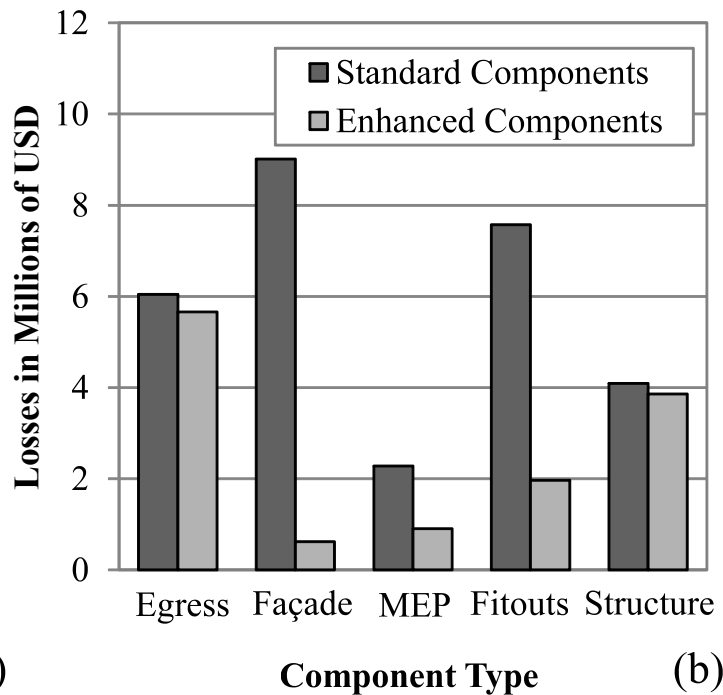
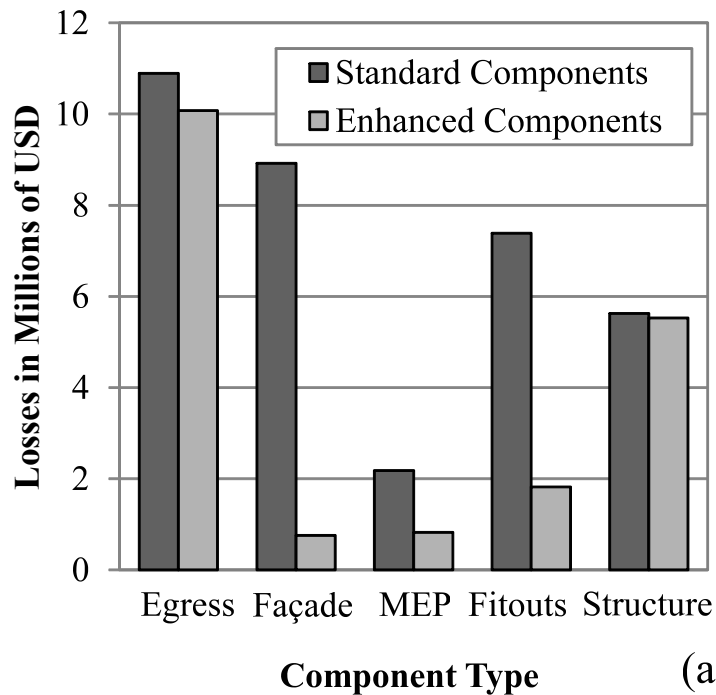
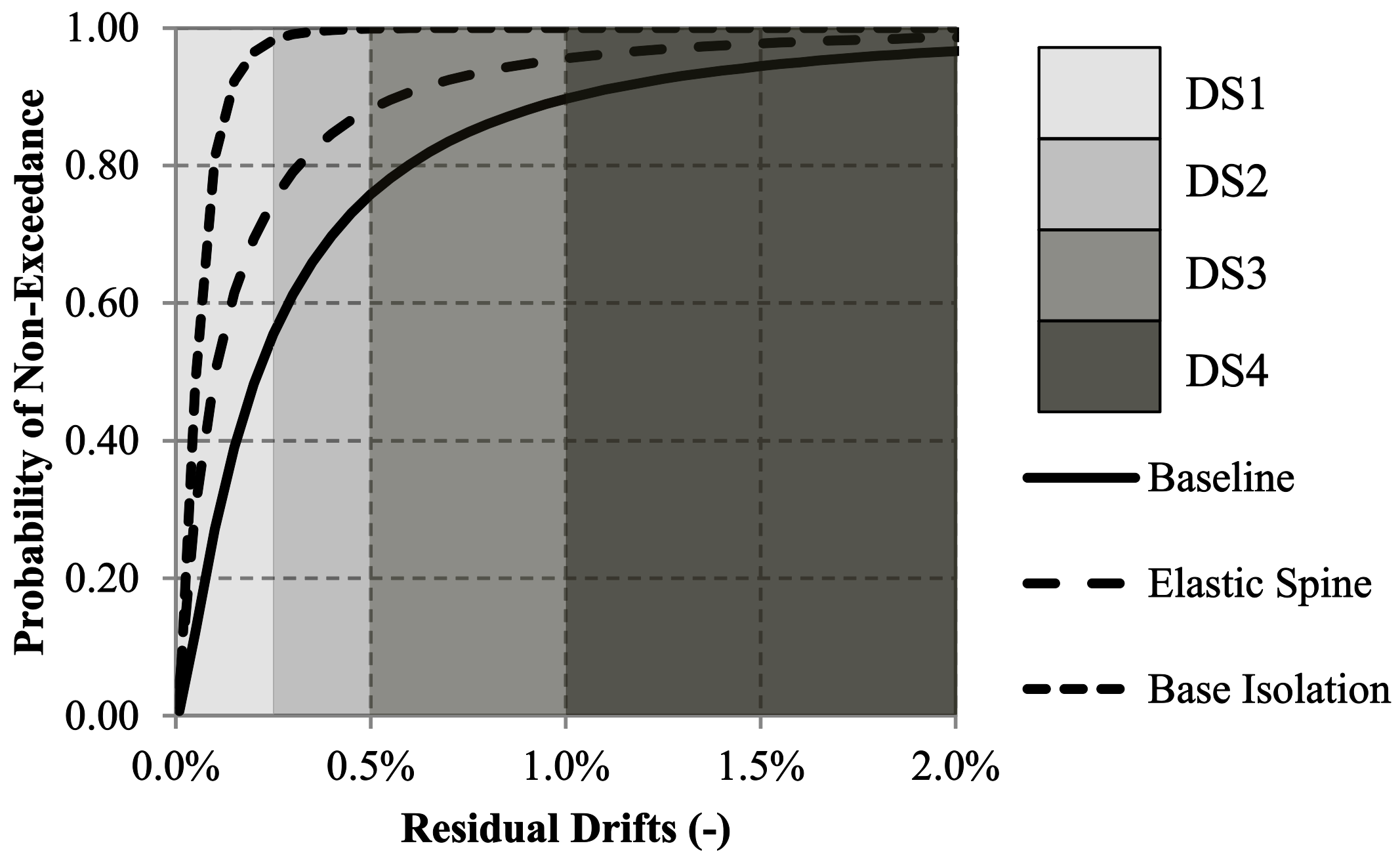
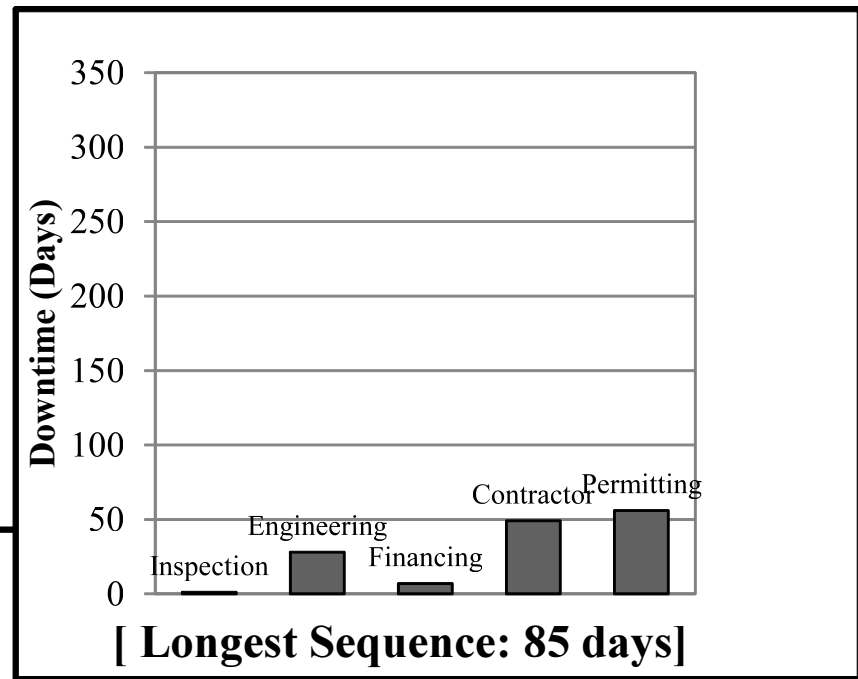
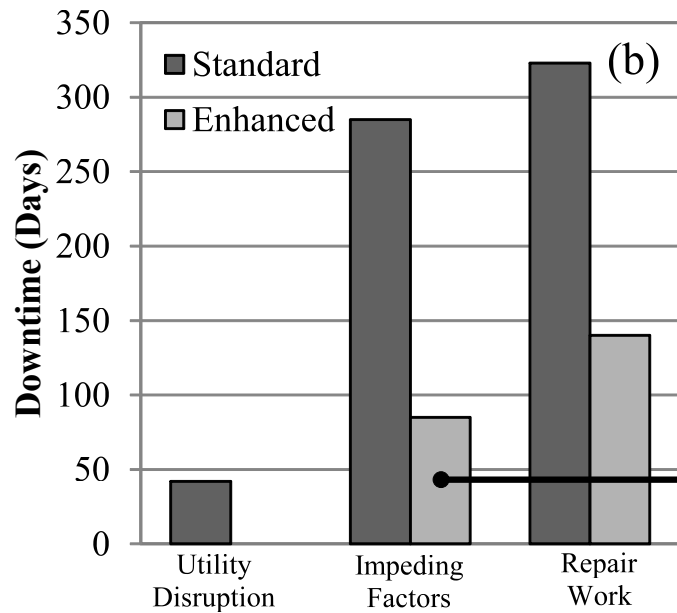
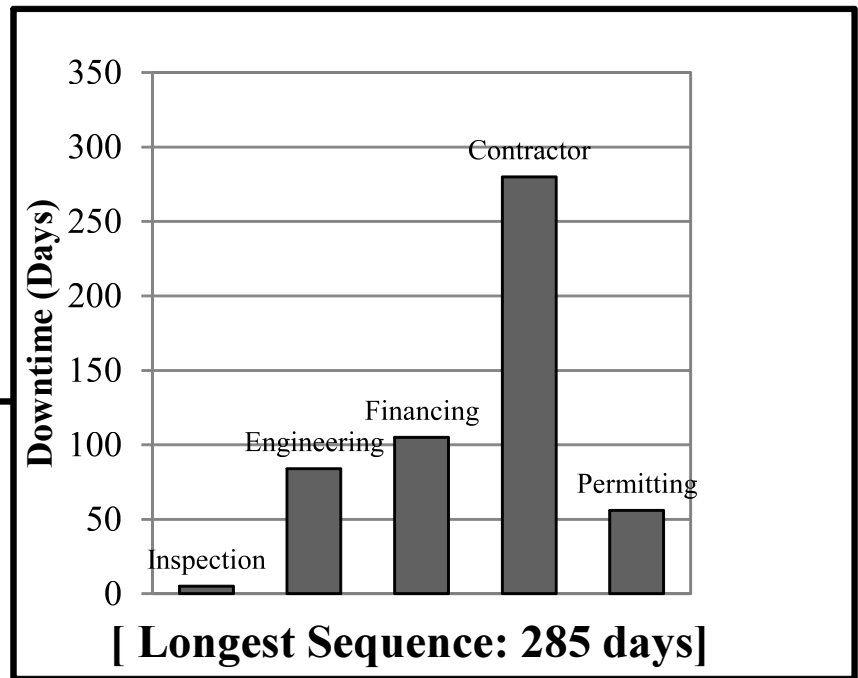
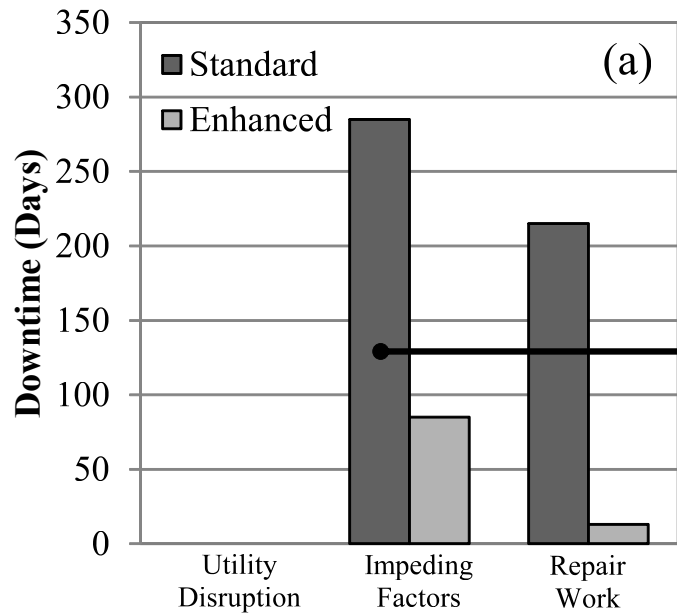


Figure 10
[Click here to download Figure: Figure_10.pdf](#)





1 **Fig 1.** Number of tall buildings built in San Francisco per decade between 1900 and 2010 (a)
2 and lateral system types for tall buildings built between 1960 and 1990 (b).

3

4 **Fig 2.** Prototype 40-story office building plan (a) and isometric (b).

5

6 **Fig 3.** Typical details observed in existing building drawings: plan section of typical moment
7 connection (a), elevation of typical moment connection (b) and typical splice (c).

8

9 **Fig 4.** Mean of maximum and minimum demand response spectra and individual components
10 for short (a) and long (b) period suites of ground motions.

11

12 **Fig 5.** Compliance with ASCE 7-10 for site specific ground motions.

13

14 **Fig 6.** Loss and downtime assessment methodology. Adapted from REDi.

15

16 **Fig 7.** Demand parameters for the archetype building (a), elastic spine retrofit scheme (b) and
17 base isolated retrofit scheme (c): transient and residual drifts (IDR) and accelerations (A) at
18 each story in each building direction.

19

20 **Fig 8.** Loss estimates for archetype building (baseline), elastic spine and base isolation
21 schemes with standard and enhanced non-structural components with (a) and without (b)
22 consideration of residual drifts.

23

24 **Fig 9.** Contribution to losses of building components for archetype building (a), elastic spine
25 retrofit (b) and base isolated retrofit (c) with standard and enhanced non-structural
26 components.

27

28 **Fig 10.** Probability distribution of residual drifts for archetype building (baseline), elastic
29 spine and base isolation retrofit schemes and associated damage states per FEMA P-58
30 (2012).

31

32 **Fig 11.** Downtime contributors for re-occupancy (a) and functional recovery (b) and sample
33 disaggregation of impeding factors for the archetype building using standard non-structural
34 components and no mitigation measures to minimize impeding factors versus enhanced non-
35 structural components and mitigation measures to minimize impeding factors.

36